Potential Association Between the Low-Energy Plasma Structure and the Patchy Pulsating Aurora

Jun Liang[1]*, Y. Nishimura[2], E. Donovan[1], B. Yang[1] and V. Angelopoulos[3]

[1]*Department of Physics and Astronomy, University of Calgary, Calgary, AB, Canada,* [2]*Department of Electrical and Computer Engineering and Center for Space Sciences, Boston University, Boston, MA, United States,* [3]*Institute of Geophysics and Planetary Physics, University of California, Los Angeles, Los Angeles, CA, United States*

While the pulsating auroral phenomena have been recognized and studied for decades, our understating of their generation mechanisms remains incomplete to date. In one main class of pulsating auroras which is termed "patchy pulsating auroras" (PPA), the auroral patches are found to basically maintain their shape and size over many pulsation cycles. Also, PPAs are repeatedly found to essentially co-move with the ExB convection drift. The above properties led many researchers to hypothesize that PPA might connect to a structure of enhanced cold plasma in the magnetosphere. In this study, we review the existing evidence, and provide new perspective and support, of the low-energy plasma structure potentially associated with PPA. Based on observations from both the magnetosphere and the topside ionosphere, we suggest that ionospheric auroral outflows might constitute one possible source mechanism of the flux tubes with enhanced low-energy plasma that connect to the PPA. We also review the existing theories of pulsating auroras, with particular focus on the role of low-energy plasma in these theories. To date, none of the existing theories are complete and mature enough to offer a quantitatively satisfactory explanation of pulsating auroras. At last, we suggest a few future research directions to advance our understanding of pulsating auroras: a) more accurate measurements of the cold plasma density, b) more developed theories of the underlying mechanisms of ELF/VLF wave modulation, and c) auxiliary processes in the topside ionosphere or near-Earth region accompanying pulsating auroras.

Keywords: pulsating aurora, low-energy plasma, auroral patch, wave-particle interaction, ionospheric outflows

1 INTRODUCTION

Pulsating aurora is an auroral form that undergoes quasi-periodic fluctuations in intensity (Johnstone, 1978). The period typically ranges from few seconds to tens of seconds (Royrvik and Davis, 1977; Yamamoto, 1988). Pulsating auroras are often observed in the equatorward portion of the auroral oval, and mainly occur in postmidnight-morning sectors and during late substorm expansion and recovery phases, but can persist for longer than individual substorm (e.g., Jones et al., 2011; 2013). Pulsating aurora is often organized in "patches," the size of which typically lies in the range of a few tens up to ~100 km in extent when mapped to ionospheric altitudes. The ultimate source of pulsating aurora is thought to be magnetospheric electrons with energies of a few keV to several tens of keV (Sandahl et al., 1980; McEwen et al., 1981; Miyoshi et al., 2010; Samara et al., 2010, 2015; Jaynes et al., 2013), though in some events the precipitation may also involve a portion of

electrons with energies as low as <1 keV (Liang et al., 2016) or as high as the relativistic energy range (Miyoshi et al., 2015). While there are other proposals of the driving mechanism of pulsating auroras (e.g., Sato et al., 2015; Mozer et al., 2017), the wave-particle interaction and its resulting pitch-angle scattering of energetic electrons in the equatorial magnetosphere remain to be the top candidate and most recognized mechanism underlying pulsating auroral precipitation. The lower-band whistler-mode chorus is usually the dominant wave mode at play in many cases (Miyoshi et al., 2010, 2015; Nishimura et al., 2010, 2011a, 2011b; Ozaki et al., 2015, 2018; Kasahara et al., 2018; Hosokawa et al., 2020), while the upper-band chorus (Nishiyama et al., 2011) and electron-cyclotron-harmonic (ECH) waves (Liang et al., 2010; Fukizawa et al., 2018) may also contribute in some events. For comprehensive reviews of pulsating auroras, see Lessard (2012) and most recently Nishimura et al. (2020).

Pulsating auroral features exhibit diverse characteristics, varying in terms of shape, size, brightness, altitude, spatial stability, modulation, lifespan, and velocity. In recent years, based on ground-based all-sky-imager (ASI) data the pulsating auroras are categorized into patchy pulsating auroras (PPA), patchy diffuse auroras (PDA), and amorphous pulsating auroras (APA), according to their morphology (Grono et al., 2017; Grono and Donovan, 2018, 2019, 2020; Yang et al., 2019). PPA is the classical type of pulsating auroras; it represents a highly structured patch that can persist for many minutes and pulsate over much of its area. PDA is similar to PPA but does not oscillate in brightness. While PDA is not "pulsating," it closely resembles PPA in terms of its spatial characteristics and occurrence distribution (Grono and Donovan, 2020). In some events, the same spatial structure is found to switch from pulsating to non-pulsating auroras (or vice versa). One such example is given in **Supplementary Material**, from which one can see that the auroral patch shifts from pronouncedly pulsating to virtually non-pulsating, yet basically maintains its structural shape. Their morphology in the ionosphere suggests that these two auroral types might be similar in generation mechanisms except for the presence/absence of modulation in precipitation. On the other hand, APA is a more dynamic pulsating auroral type with rapidly changing shapes and locations, yet lacking repeatable patch structures between successive images captured at a 3-sec cadence of THEMIS ASI. The motion of APA is more dynamic than PPA and seems unrelated to E × B drift. There is a possibility that APA could arise from time-aliasing of rapidly-propagating pulsating aurora with "streaming" behavior and pulsations faster than 3-sec, the sampling rate of THEMIS ASI (Nishimura et al., 2020). Statistically, the occurrence distributions of PPA and APA tend to map to different regions in the equatorial magnetosphere (Grono and Donovan, 2020), and there is evidence that the PPA and APA are likely associated with different energy ranges of electron precipitation (Yang et al., 2019; Tesema et al., 2020). It is thus reasonable to speculate that their generation mechanisms may be different. Most importantly, based upon phenomenological evidence there is no concrete rationale to conceive a link between the APA and enhanced cold plasma in the magnetosphere. In this paper, we shall mainly focus on the PPA type and explore the possible mechanism underlying its

resilient spatial shape. For this research purpose, we examine all the studies to be referred to in this review, as long as the optical data are involved and available, to check whether their investigated pulsating auroral events are PPA or APA, based on established techniques and criteria in distinguishing the two types (Grono et al., 2017; Grono and Donovan, 2018; Yang et al., 2019) according to the cadence rate of available optical instruments.

One striking characteristic of PPA is that it can basically maintain its size shape through many cycles of pulsations (Scourfield et al., 1972; Johnstone, 1978; Humberset et al., 2018). Furthermore, it has often been noted that the motion of the overall PPA essentially conforms to the E × B convection drift (Davis, 1971; Nakamura and Oguti, 1987; Royrvik and Davis, 1977; Scourfield et al., 1983; Yang et al., 2014; 2017; Takahashi et al., 2019). The above two key features of PPA will be further elucidated with the most recent observations in **Section 2**. In a mathematical form, the spatiotemporal behaviors of a PPA can be approximately written as (e.g., Kangas and Cao, 1995):

$$P(\mathbf{r}, t) = f(t) \cdot g(\mathbf{r} - \mathbf{v}_E t) \tag{1}$$

in which $f(t)$ depicts the temporal modulation, and $g(\mathbf{r})$ depicts the spatial shape of the PPA. V_E denotes the E × B drift speed. The relation between the patch motion and E × B drift invalidates the scenario that the PPA shape maps to an energetic electron structure at the magnetic equator, whose gradient/curvature drift speed would usually by itself exceed the E × B drift in the near-Earth magnetosphere, and whose energy dispersion led by the gradient/curvature drift would tend to quickly deform the patch (Yang, 2017).

The above salient features of PPA has led many researchers to hypothesize that PPA might connect to a structure of enhanced "cold" plasma in the magnetosphere (Johnstone, 1978; Oguti, 1976; Davidson and Chiu, 1987; Davidson, 1990, Demekhov and Trakhtengerts, 1994; Tagirov et al., 1999; Liang et al., 2015; Nishimura et al., 2015). A brief discussion of the existing theories of pulsating auroras with be given in **Section 4**. In a nutshell, the classical theoretical view of pulsating auroras is that each luminous patch in the ionosphere represents the magnetic mapping of a region of enhanced cold plasma density near the equatorial plane. The gradient/curvature drift of energetic electrons brings fresh precipitation material into the regions of enhanced plasma density. The interaction between the drifting energetic electrons, the ambient cold plasma, and the ELF/VLF waves—though the details of such an interaction differ from theory to theory—lead to modulated scattering of energetic electrons into the loss cone within the area of each enhanced-density zone, resulting in an oscillatory precipitating flux having the outline of the plasma blob. In plasma physics, the definition of "cold" or "hot" particles is contingent upon the research objective and especially the reference plasma population they are compared to. In the context of pulsating auroral studies, a particle population is characterized as cold when: a) its energy is much lower than that of the thermal electron/ion population in the central plasma sheet (CPS) region; b) its energy range is lower

than the minimum resonant energy of the wave-particle interaction at play, and c) its gradient/curvature drift speed is distinctly smaller than the ambient E × B velocity. In the inner CPS, electrons with energy <~100 eV and ions with energy <1 keV would usually satisfy the above criteria and can be deemed "cold." Under such a definition the so-called "warm plasma cloak" (Chappell et al., 2008), which is warmer compared to the plasmaspheric population, would also be considered as "cold" population here. In the near-Earth CPS, such cold electron/ions are often distinctly separated from the thermal and suprathermal plasma sheet populations in terms of energy range, pitch-angle distribution, drift speed and trajectory, and source mechanisms [e.g., Wang et al. (2012); Delzanno et al. (2021)]. In this paper, we shall use the term "low-energy plasma" to denote the cold electrons and ions in the above-depicted sense. Such a low-energy plasma would not directly resonate with the waves by itself, but could form an ambient structure that can significantly affect the excitation/propagation of the waves within it (Cuperman and Landau, 1974; Li et al., 2011b; Wu et al., 2013; Katoh, 2014; Hanzelka and Santolik, 2019; Ke et al., 2021). We should also note that, while the notion that PPA is associated with a density enhancement structure was more often suggested, it is also possible that the PPA might be associated with a density depletion structure, since the density depletion structure may also affect the amplification/propagation of the whistler-mode chorus inside it [e.g., Wu et al. (2013); Li et al. (2011b); Katoh (2014)].

Of course, while **Eq. 1** offers an approximate depiction of the general characteristics of PPAs, a number of complications/exceptions may exist. First, the patch size is certainly not rigorously fixed over time (Humberset et al., 2016; 2018; Bolmgren, 2017; Partamies et al., 2019). Secondly, the PPA may have intra-patch sub-structures and fine-scale variations. For example, some of the patches may feature a "streaming/expansion" behavior, namely that the entire patch is not switched on/off simultaneously; instead, it grows from a portion and rapidly expands to its full extent during the on-time, followed by a retraction in the area as the pulsation switches off (Royrvik and Davis, 1977; Yamamoto, 1988; Tagirov et al., 1999). Using high-resolution imagers Nishiyama et al. (2016) investigated the sub-structures within a pulsating auroral patch. They found that the sub-structures smaller than ~20 km feature rapid back and forth fluctuations relative to the larger patch whose drift is much slower and steady. These rapid, intra-patch variations of pulsating auroras are almost certainly led by physical processes other than cold plasma [e.g., Fukuda et al. (2016)]. With the above complications in mind, and realizing that cold plasma is certainly not the only factor in controlling the spatiotemporal variations of pulsating auroras, in this paper we shall nevertheless focus on the role of low energy plasma in producing the overall patch shape, and leave the intra-patch fine structures, the fast motion of patches (e.g., streaming) and the subtleties in ionospheric electrodynamics for separate studies.

One other area of important new findings of pulsating auroras in the last decade, thanks to the deployment of high-time-resolution imagers, is the details of rapid modulation embedded in each on-time, and the subtleties and high variabilities in the on- and off-time durations, of pulsating

auroras [e.g., Samara et al. (2010); Nishiyama et al. (2014; 2016); Humberset et al. (2016); Dahlgren et al. (2017)]. Though those fine-scale temporal characteristics are not of the core interest of this review, some of the results may also shed light on the possible role of low-energy plasma in pulsating auroras. For example, based on the observation that the on-off pulsation periods showed no significant correlations with auroral brightness, Nishiyama et al. (2014) suggested that variations in the cold plasma density play a dominant role in controlling the conditions of wave-particle interactions that have temporal scales of the on-off pulsation periods. On the other hand, Humberset et al. (2016) claimed that there is no clear candidate of the suggested mechanisms and drivers to explain the observational constraints set by the PPAs in a satisfactory manner, based on their observed temporal characteristics and energy deposition of PPAs.

While the speculation regarding PPA-associated cold plasma structure has existed for decades, it is fair to state that, the speculation still needs further investigation and validation to date. This is mainly due to two reasons: 1) the experimental difficulty in reliable measurements of cold plasma density as well as the shape and motion of the cold plasma in the magnetosphere; 2) the difficulty in establishing conjugacy between the magnetospheric *in-situ* probes and an individual PPA. That being said, certain progress has been achieved, thanks to the global deployment and technological advances of both ground-based and *in-situ* instruments/missions in the past couple of decades. Furthermore, a number of recent findings of pulsating auroras, though by themselves not directly observing low-energy plasma, may impose certain useful implications and constraints on the characteristics of the low-energy plasma associated with pulsating auroras. In this paper, we shall review existing observational evidence and theoretical consideration of the potential association between the low-energy plasma and the PPA. The rest of the paper is arranged as follows. In **Section 2** we shall first review some most recent reports on the shape persistence and overall motion speed of PPA. We shall then review existing *in-situ* observational evidence of low-energy plasma in potential association with PPA in **Section 3**. In **Section 4** we shall review some existing theories of pulsating auroras, with particular focus and comments on the role of low-energy plasma in these theories. **Section 5** concludes this paper, in which we also suggest a few future tasks to advance our understanding of pulsating auroras.

2 PATCHY PULSATING AURORA: RESILIENT PATCH SHAPE AND E × B DRIFT SPEED

As mentioned above, historically, the hypothesis that PPA might map to an enhanced cold plasma region stemmed from the long-standing observations that PPA features a resilient patch shape over many pulsations, and that the overall apparent motion of the patch is consistent with the E × B convective drift. In this section, we shall review some of the recent observations in the above regard, to prepare the context for a subsequent review of the *in-*

situ evidence of low-energy plasma potentially associated with PPA.

2.1 Persistence and Subtle Change of Patch Size

While the persistence in patch shape has long been known to be a key feature of PPA, in many previous works the above notion was qualitatively inferred from a visual browse of PPA over many pulsations by researchers. In recent years, quantitative and objective algorithms have been developed to discern repetitive PPA events (Grono et al., 2017), and to examine the persistence as well as gradual changes of the patch shape and size (Humberset et al., 2016, 2018; Bolmgren, 2017; Partamies et al., 2019). Individual patch sizes typically range from several hundred to a few thousand km², as inferred from existing studies and our experience with PPA. Using ASI data at Poker Flat Research Range, Alaska, Humberset et al. (2018) carefully examined the extent to which pulsating auroral patches maintain their morphology and fluctuate in a coherent fashion. They found that, for the PPA events they investigated the patch shape can be considered remarkably persistent with 85–100% of the patch being repeated for 4.5–8.5 min, while the total lifetime that the patch structure is discernible in the ASI FOV is ~7–11 min. While Humberset et al. (2018) did not explicitly calculate the change rate of the patch area, it can be inferred from their presented results (e.g., their **Figure 9**) that: a) Patch 1 appears to show a trend of slightly increasing size, largely due to a slight broadening in east-west extension. b) The other three patches generally show a trend of decreasing patch size, but the average decay rate is estimated to be no more than a few tens of km²/min, as compared to the ~1,000–4,800 km² patch area in their events. Bolmgren (2017) and Partamies et al. (2019) investigated the patch size evolution based on a large dataset of pulsating aurora events from the MIRACLE network in northern Fennoscandia. Their technique did not track individual patches. Instead, they studied the average time-dependent trend of the total patch size, defined as the total area of all discernible patches within the ASI FoV, and the average patch size per frame image, defined as the total patch area divided by the number of patches. Bolmgren (2017)'s study focused more on the frame-averaged patch size. They found that most events show a stable or decreasing patch size, yet a small percentage of events show a trend of slightly increasing size. The patch decay rate typically ranges from a few km²/min up to few tens of km²/min. Partamies et al. (2019) also noticed that there are more events showing a decreasing patch size than events showing an increasing patch size. Based on a selected subset of events that show a consistently decreasing trend of patch size, Partamies et al. (2019) found the event-averaged decay rate of the total patch area is mostly within ~10–40 km²/min. Given the fact the total patch area defined in Partamies et al. (2019) may often contain multiple patches (see their examples) which are uncorrelated with each other, the above decay rate of the total patch area can be considered as the upper limit of the decay rate of an individual patch. To summarize from the above studies: 1) the PPA patch shape and size can be resilient over many minutes, yet slowly changes with time; 2) there are more events showing a stable or overall decreasing patch size than events showing an increasing patch size; 3) the patch decay rate is most likely in the range between a few km²/min and a few tens of km²/min. The slow change of patch shape/size may allude to the time evolution of the low-energy plasma structure in the magnetosphere, e.g., led by the energy dispersion (Yang, 2017).

2.2 Patch Drift Speed

Ever since the recognition of pulsating auroral phenomena, it has been suggested that the motion of the pulsating auroral patch could be caused by convection drift in the magnetosphere (Johnstone, 1978). Akasofu et al. (1966) first noticed that auroral patches drift eastward in the morning sector at typical speeds of a few 100 m/s. Nakamura and Oguti (1987) found that the overall drift pattern of auroral structures derived from all-sky TV observations was very similar to the ionospheric convection pattern measured by radars and satellites, but the comparison was not based upon the data during the same time intervals. Using observations from Scandinavian Twin Auroral Radar Experiment and simultaneous sequences of auroral images in one event, Scourfield et al. (1983) noticed that motion of pulsating aurora patches is basically consistent with E × B drift velocity.

A more systematic and definitive comparison study between the motion of PPA patches and the local E × B drift velocities was done by Yang et al. (2014). Five PPA patches were identified in data obtained from the THEMIS ASI at Gillam, while the collocated E × B convection velocities were inferred from the Super Dual Auroral Radar Network (SuperDARN) data. Yang et al. (2014) found that azimuthal velocities of five patches derived from THEMIS ASI data were consistent with the local convection velocities obtained from SuperDARN. Yang et al. (2014) also compared the PPA velocity with the Swarm satellite observations of ion drifts (Knudsen et al., 2017) in the upper F-region ionosphere. Notwithstanding the uncertainty in both measurements, the east-west patch velocities were found to be within ~20% difference from the cross-track ion drifts measured by the Swarm satellite. In particular, the trend of the latitudinal variations of ion drifts is reproduced in changes of the motion velocities of the patches at different latitudes. Based upon an extensive database obtained from THEMIS ASI over 7 years, Yang et al. (2017) made a statistical survey on the east-west motion of PPA patches. Their results showed that PPA patches mainly drift eastward after midnight and drift westward before midnight, compatible with the general pattern of global convection, and that the patch velocities are in the range of convection velocities expected from empirical convection models given the magnetic latitude. This result also indirectly supports the idea that the patch motion is convection.

However, Humberset et al. (2018) found that in some cases the patch motion differed from the E × B drift locally measured in the ionosphere by SuperDARN. We note that the velocity level (~50–100 m/s) in their events is below average for PPAs (Yang et al., 2017), and is relatively difficult to be accurately measured by SuperDARN. Humberset et al. (2018) admitted the possible uncertainty in the SuperDARN velocities, and allowed for the possibility that the patches might indeed move with E × B drift. One other possible reason for the discrepancy might be that the

local electric field is modified by the ionospheric electrodynamics (e.g., polarization electric field) associated with the pulsating auroral precipitation (Hosokawa et al., 2008, 2010; Takahashi et al., 2019), and thus differs from the magnetospheric flux tube convection.

Takahashi et al. (2019) investigated the motion of PPA patches in an experiment using the European incoherent scatter (EISCAT) radars, Kilpisjärvi Atmospheric Imaging Receiver Array (KAIRA), and an all-sky imager simultaneously. One notable advantage of Takahashi et al. (2019) study over the above-mentioned studies using SuperDARN radar lies in that, Takahashi et al. (2019)'s multi-instrumental measurements offered height information of ion velocities. Their results showed that the electric field estimated from the drift speed of auroral patches approximately corresponded with the convective electric field derived from EISCAT and KAIRA, indicating that the motion of these auroral patches was overall governed by the magnetospheric convection, though height-dependent subtle variations due to the polarization electric field generated within the patch exist.

3 EXISTING OBSERVATIONS OF LOW-ENERGY PLASMA ASSOCIATED WITH PPA

In this section, we shall review existing reports of the *in-situ* observations of low-energy plasma potentially associated with pulsating auroral activities. Some new perspectives and datasets complementary to the existing studies will be introduced. It should be noted that in some of the studies, such as Li et al. (2011b) and Nishimura et al. (2015), their research focus is on the modulation of whistler-mode chorus waves based on *in-situ* measurements, yet without conjugate optical observations. However, given the notion that the pulsating auroras could be the direct consequence of the quasi-periodic modulation of the whistler-mode chorus, their studies are still deemed relevant to our research objective, though it is impossible to check whether the hypothesized pulsating auroras are of PPA or APA types.

3.1 Low-Energy Electron Observations From *In-Situ* Particle Measurements

Nemzek et al. (1995) compared the ground optical observations of pulsating auroras and the *in-situ* measurements of high-energy electrons and low-energy plasma obtained from Los Alamos National Laboratory (LANL) geosynchronous satellites, and then examined the observations against the existing theoretical models of pulsating auroras proposed by Davidson and Chiu (1987) and Demekhov and Trakhtengerts (1994). Nemzek et al. (1995) found that, for most events, the upper limit of the plasma density was ≤ 1–$2 \, cm^{-3}$, and they could not identify any clear dependence between the *in-situ* plasma density and the pulsating auroras. They however admitted that contaminations from high-energy penetrating particles in their dataset hindered a more reliable evaluation of the local plasma density in many of their

events. It should also be noted that, Nemzek et al. (1995) did not examine exact conjugacy between the geosynchronous probe and individual auroral patches. Their conjugacy condition and measurements were relevant to extended intervals of overall pulsating auroral activities that presumably contained many individual patches stochastically passing over the satellite footprint in the ionosphere. Nemzek et al. (1995) did notice that there are some small and rapid increases in density which had apparent spatial scales (a few tens to hundreds of km when mapped to the ionosphere) similar to those of individual pulsating auroral patches. However, the relative density enhancement over the background was found to be on the order of ~10% only. Nemzek et al. (1995) thus suggested that plasma density enhancement (inside-outside enhancement ratio ≥ 1) required by Demekhov and Trakhtengerts (1994)'s flow-cyclotron-maser model might not be realistic, yet the minimum change in plasma density as proposed in the Davidson and Chiu (1987) relaxation oscillator model seems to be supported. Due to the lack of their optical data source, we cannot check whether their investigated pulsating auroras events belonged to PPA or APA type.

Nishimura et al. (2015) noticed the existence of low-energy (<20 eV) field-aligned electrons in their chorus modulation events, together with the low-energy (~100 eV) field-aligned ions (to be discussed in detail later in **Section 3.4**). However, the observable part of the field-aligned electrons reported in Nishimura et al. (2015) was found to be barely above the spacecraft potential, making it very difficult to directly infer the electron density contained in such field-aligned electron beams—their authors actually resorted to low-energy ions to estimate the cold plasma density, as we shall highlight later in this section.

Samara et al. (2015) investigated both the high-energy (>1 keV) and low-energy (<1 keV) electron features associated with pulsating auroras based on low-Earth-orbit (LEO) observations from the Defense Meteorological Satellite Program (DMSP) satellites and the Reimei satellite. The downgoing low-energy electrons in their observations were interpreted as the interhemispherically transported secondary electrons [e.g., Khazanov et al. (2014)] produced by the primary pulsating auroral precipitation. Upon examining their events, we note that their Event three to six appear to be most pertinent to the PPA type. Samara et al. (2015) found a trend of the reduction of low-energy electron precipitation corresponding to the pulsating aurora, and interpreted that such a reduction of low-energy electrons is consistent with the strongly temporally varying pulsating aurora being associated with upward field-aligned currents and hence parallel potential drops of up to ~1 kV, which blocks the secondary electrons from escaping the ionosphere. Under such a notion, Samara et al. (2015)'s results might allude to a possible depletion of low-energy electron density in the pulsating auroral flux tubes. However, the reduction of low-energy electron precipitation did not occur in every PPA event; it is not evident, for example, in their Event 5. Also, it should be noted that the instrumental limitation prevents their authors to examine the electron features at energies lower than a few tens of eV.

3.2 Plasma Density Measurement From Other Techniques

Li et al. (2011b; 2013) investigated the modulation of whistler-mode chorus intensity by cold electron density variations inferred from spacecraft potentials of THEMIS satellites at the equatorial magnetosphere (Angelopoulos, 2008). They found that the chorus intensity modulation is frequently strongly correlated with electron density variations, either a density enhancement or a density depletion. In terms of their occurrence distribution, the density depletion events mostly occur in the midnight-postmidnight sector, and may also be occasionally seen in the premidnight sector. In comparison, the density enhancement events mostly occur in the postmidnight-dawn sector and also in the dayside. The density depletion events extend to higher L-shells than the density enhancement events. There were no conjugate optical observations in their study. However, under the notion that the pulsating auroras could be the direct consequence of the quasi-periodic modulation of chorus waves, it is instructive to compare the equatorial occurrence distribution of PPA/APA (Grono and Donovan, 2020) with that of the density enhancement/depletion events in Li et al. (2011b). PPA tends to be closer to dawn, and limited to lower L-shells, than APA. It appears that the APA occurrence distribution mostly overlaps with that of the density depletion events, while the PPA occurrence contains a mixture of density enhancement and depletion events. Upon comparing with the Electrostatic Analyzer (ESA) measurements onboard THEMIS, Li et al. (2011b) noticed that electron fluxes at low energies (<a few 100 eV) and with field-aligned anisotropy increase correspondingly in density enhancement events, but no corresponding electron flux variation is identified for density decreases events in the measurable energy channels of ESA. There are two possibilities. 1) The changes in the electron population in the density depletion events likely occur at energy lower than the instrumental limit (~10 eV for THEMIS ESA). 2) The satellite potential from which Li et al. (2011b) inferred the electron density might contain an artificial effect because of photoelectron escaping due to intense chorus electric fields (Malaspina et al., 2014). With the possible artifact in density depletion events in mind, and by noting the similarity between the density enhancement events and PPAs in terms of their occurrence distribution, the density enhancement in Li et al. (2011b) appears to constitute a slightly more credible (i.e., with measurable and corroborative particle counterparts) source for some PPAs, though the existence of density-depletion events and their potential role in some pulsating auroras (including APA) cannot be excluded.

Nishiyama et al. (2011) adopted an indirect yet creative approach to estimate the cold plasma density in the equatorial source region of pulsating auroras. Their technique is based on Reimei satellite observations and a time-of-flight analysis of the energy dispersion of precipitating electrons (Miyoshi et al., 2010). They found that the equatorial cold plasma density ranges from 0.2 to 21.7 cm^{-3} in their events and tends to increase as the source region moved toward the Earth. Nishiyama et al. (2011) did not provide the full event list of their study, but their presented event examples appear to be PPA. Since their technique is applicable only during the on-time of an active pulsating aurora, it is difficult to evaluate whether their inferred cold plasma density represents an enhancement or depletion compared to the ambient plasma density. Nevertheless, the inferred plasma density was found to be generally compatible with the results of empirical models [e.g., Carpenter and Anderson (1992); Sheeley et al. (2001)], implying that a strong enhancement of cold plasma density in the pulsating auroral flux tube required by the Demekhov and Trakhtengerts (1994) model might not be achievable, consistent with Nemzek et al. (1995)'s conclusion.

3.3 Low-Energy Ions From LEO Satellite Observations

The difficulty in reliably measuring cold electrons from *in-situ* particle data impelled some researchers to look into the low-energy ion structures. Liang et al. (2015) investigated 28 event intervals and 54 pulsating auroral patches that were crossed by LEO satellites. Their event selection criteria, such as that the pulsating aurora patch must be repetitively active in 2-min surrounding the passage of the LEO satellite, implies that the pulsating auroral events studied in Liang et al. (2015) were predominantly the PPA type. We have carefully re-examined all the events in Liang et al. (2015). Using the discrimination criteria in Grono et al. (2017) and Yang et al. (2019), we confirm that 47 pulsating auroral events in Liang et al. (2015) are indeed PPAs, while the rest seven events may be questionable or better categorized as APA. In 33 out of the 47 PPA events, the PPA is found to be co-located with a particle structure with enhanced low-energy ion fluxes. These low-energy ion structures are usually energy-band limited, with core energy ranging from several tens of eV up to a few hundred eV. Their pitch-angle distribution is more or less isotropic in precipitating directions within the loss cone, yet tends to peak at oblique and/or quasi-perpendicular pitch angles. On the other hand, the distribution consistently shows a sharp cut-off beyond 90° pitch angle, indicating a small upgoing flux in all events. Therefore, those low-energy ion structures must come from higher altitudes above the LEO satellite. Those PPA-associated low-energy ion structures are located equatorward of the precipitation boundary of CPS thermal ions, conformal to the normal geometry of PPA with respect to the CPS ion precipitation boundary (Viereck and Stenbaek-Nielsen, 1985; Grono and Donovan, 2019). Based upon the above observations, Liang et al. (2015) suggested that the observed low-energy ion structure might owe its origin to the ion outflows from the ionosphere. The outflows from the ionospheres in both hemispheres may populate the magnetospheric flux tubes with the low-energy plasma, particularly during disturbed intervals. The flux tubes filled with enhanced low-energy plasma of ionospheric origin define the PPA region, when the other prerequisites of PPA are also met, i.e., energetic electron fluxes and ELF/VLF waves.

Not all the pulsating auroral events investigated in Liang et al. (2015) are accompanied by discernible low-energy ion structures in LEO satellite measurements. There are a few possible explanations. 1) As we shall discuss in **Section 5**, there is a
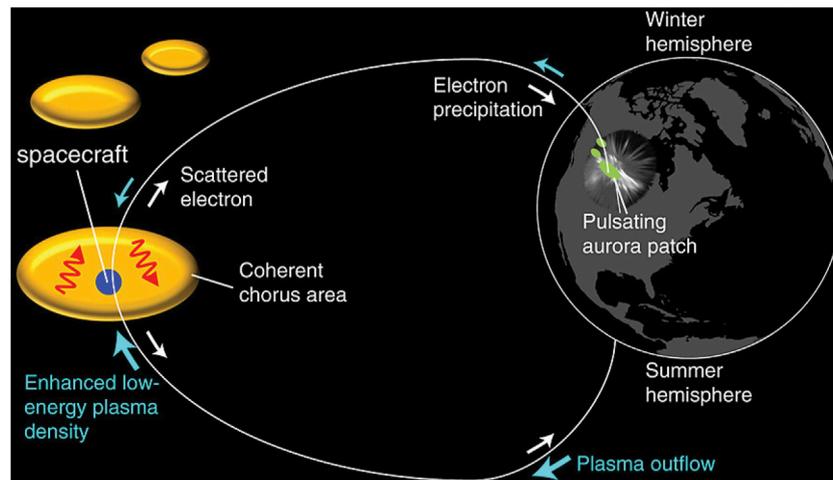
FIGURE 1 | Schematic illustration of the formation of cold plasma flux tubes from ionospheric outflows and its connection to PPA. Copied from Nishimura et al. (2015).
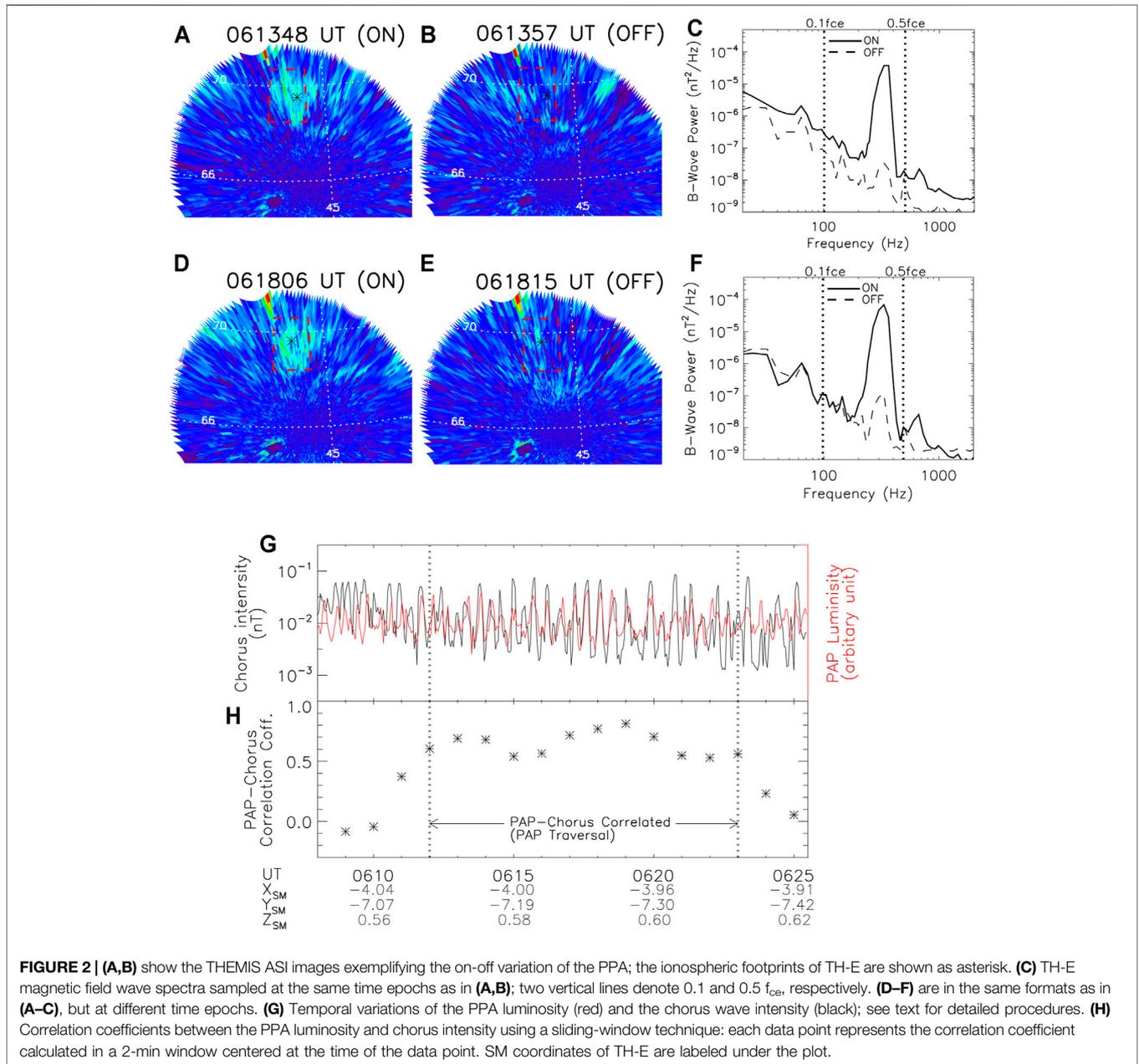
likely mixture of different types of pulsating auroras with different underlying generation/modulation mechanisms, and it is not surprising that some types of pulsating auroras are not necessarily related to a low-energy plasma structure. 2) A low-energy ion structure corresponding to the PPA may indeed exist in the magnetosphere, but does not extend to the topside ionosphere and thus cannot reach the LEO satellite. For example, the possible existence of parallel electric fields above the satellite in some events may hinder the low-energy ions from reaching the satellite. Also, contingent upon the source mechanisms of the low-energy ions and their transport history in the magnetosphere, in some events the low-energy ions could become entirely trapped in the magnetosphere and mirror at altitudes above the satellite. At last, it is also possible that in some cases the low-energy ion structure already reached the equatorial magnetosphere where the high-energy electron precipitation (and thus PPA) is produced, but has not reached the ionosphere by the time of satellite traversal, since high-energy electrons travel much faster than the low-energy ions.

3.4 Low-Energy Ions From Magnetospheric *In-Situ* Observations

Based on THEMIS observations Nishimura et al. (2015) identified in some events that low-energy ions of ~100 eV apparently modulate the whistler-mode chorus intensity. Those low-energy ions exist as a field-aligned structure, with noticeable oscillations superimposed. Such oscillations of the low-energy ion densities are found to correlate with the chorus intensity variations. Nishimura et al. (2015) also noticed the existence of low-energy (<20 eV) field-aligned electron structure together with the field-aligned ion structure, but it is difficult to reliably derive the low-energy electron density due to constraints imposed by the spacecraft potential and ESA energy range limit. The low-

energy ion beam structure is however well above the spacecraft potential and its density is relatively easy to measure. Nishimura et al. (2015) then performed a theoretical calculation of the chorus wave growth rate. Assuming charge neutrality, the low-energy ions were used to represent cold plasma density in wave growth rate calculations, and the enhancements of the low-energy plasma density were found to contribute most effectively to chorus linear growth rates. The results in Nishimura et al. (2015) demonstrated that the low-energy plasma may directly modulate the whistler-mode chorus intensity in the equatorial magnetosphere. In line with Liang et al. (2015), Nishimura et al. (2015) also proposed that ionospheric outflows are the source of the field-aligned ion structures in their observations, and that they form the flux tubes with enhanced cold plasma, which connect to the PPA.

The proposed scenario based upon the results in Liang et al. (2015) and Nishimura et al. (2015) is sketched in **Figure 1** [copied from Nishimura et al. (2015)]. The PPA mechanism involves high-energy electrons of magnetospheric origin, the low-energy plasma of ionospheric origin, and certain ELF/VLF waves (chorus waves for example in **Figure 1**). In an overlapping region of energetic electrons and low-energy plasma flux tubes filled by outflows, ELF/VLF waves can be enhanced/modulated via an interaction with the low-energy plasma and energetic electrons. Such modulated ELF/VLE waves drive the scattering and precipitation of energetic electrons and result in the PPA. Since the plasma outflows are contingent upon the ionospheric condition in the specific hemisphere (e.g., winter or summer), it is certainly possible that the density distribution of low-energy plasma could be asymmetric in the northern and southern hemispherical segments of the outflow flux tubes. This may also affect the preferential direction of wave growth and its duct-propagation inside the flux tubes. Therefore, the shape and occurrence of PPAs, when observed simultaneously in two hemispheres, may be different and non-conjugate (Sato et al., 1998; Watanabe et al., 2007).

FIGURE 2 | (A,B) show the THEMIS ASI images exemplifying the on-off variation of the PPA; the ionospheric footprints of TH-E are shown as asterisk. **(C)** TH-E magnetic field wave spectra sampled at the same time epochs as in **(A,B)**; two vertical lines denote 0.1 and 0.5 f_{ce}, respectively. **(D–F)** are in the same formats as in **(A–C)**, but at different time epochs. **(G)** Temporal variations of the PPA luminosity (red) and the chorus wave intensity (black); see text for detailed procedures. **(H)** Correlation coefficients between the PPA luminosity and chorus intensity using a sliding-window technique: each data point represents the correlation coefficient calculated in a 2-min window centered at the time of the data point. SM coordinates of TH-E are labeled under the plot.

3.5 Conjugate Magnetosphere-LEO Satellite Observations of Low-Energy Ions

One key obstacle in efforts to link magnetospheric particle features to a PPA lies in the uncertainty of magnetosphere-ionosphere mapping. It is often difficult to determine whether the *in-situ* probe is situated in magnetospheric flux tubes connecting to the PPA. To date, the most reliable technique to infer conjugacy between a magnetospheric satellite and a pulsating aurora structure in the ionosphere is via the correlation between the temporal variation of the whistler-mode chorus intensity observed by the satellite and that of the optical auroral luminosity of pulsating auroras recorded by

ground ASIs (Nishimura et al., 2010; 2011a; 2011b). In the following we shall re-investigate one of the events studied in Nishimura et al. (2011b), with new datasets and a focus on the low-energy plasma signatures associated with the PPA.

The event occurred on January 6, 2010. **Figures 2A,B,D,E** exemplify two on-off variations of the PPA of interest around 06:13:50 and 06:18:10 UT, respectively. To relieve the moonlit contamination in this event we have performed a background subtraction procedure; the "darkest" pixel frame used for subtraction is determined according to the minimum brightness within 2 min surrounding the displayed image epoch. The ionospheric footprint of TH-E based upon the mapping scheme in Nishimura et al. (2011b) is shown as an
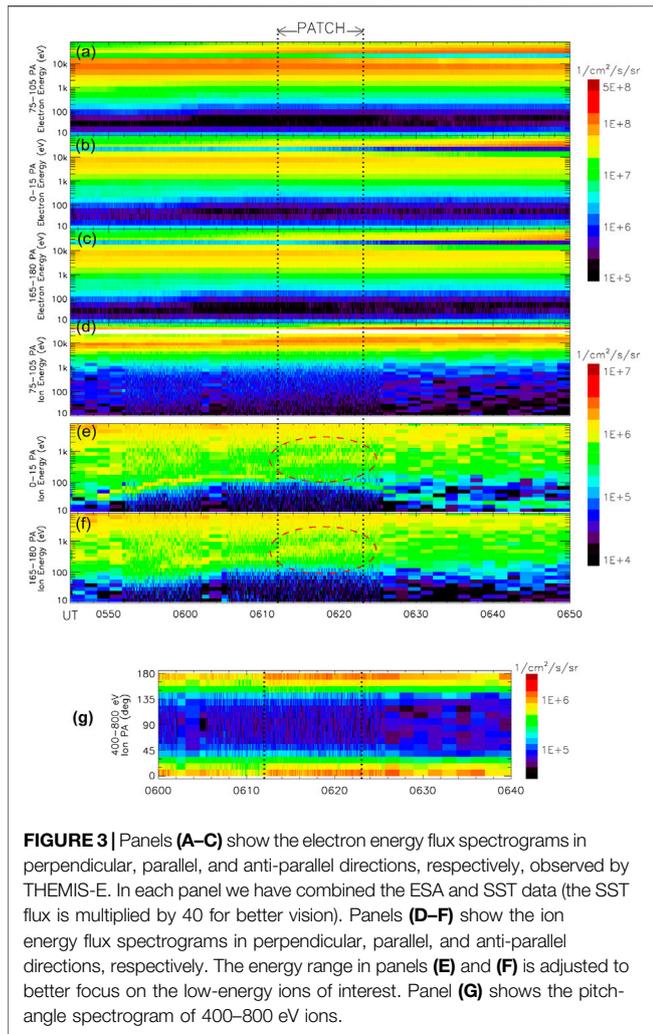
FIGURE 3 | Panels **(A–C)** show the electron energy flux spectrograms in perpendicular, parallel, and anti-parallel directions, respectively, observed by THEMIS-E. In each panel we have combined the ESA and SST data (the SST flux is multiplied by 40 for better vision). Panels **(D–F)** show the ion energy flux spectrograms in perpendicular, parallel, and anti-parallel directions, respectively. The energy range in panels **(E)** and **(F)** is adjusted to better focus on the low-energy ions of interest. Panel **(G)** shows the pitch-angle spectrogram of 400–800 eV ions.
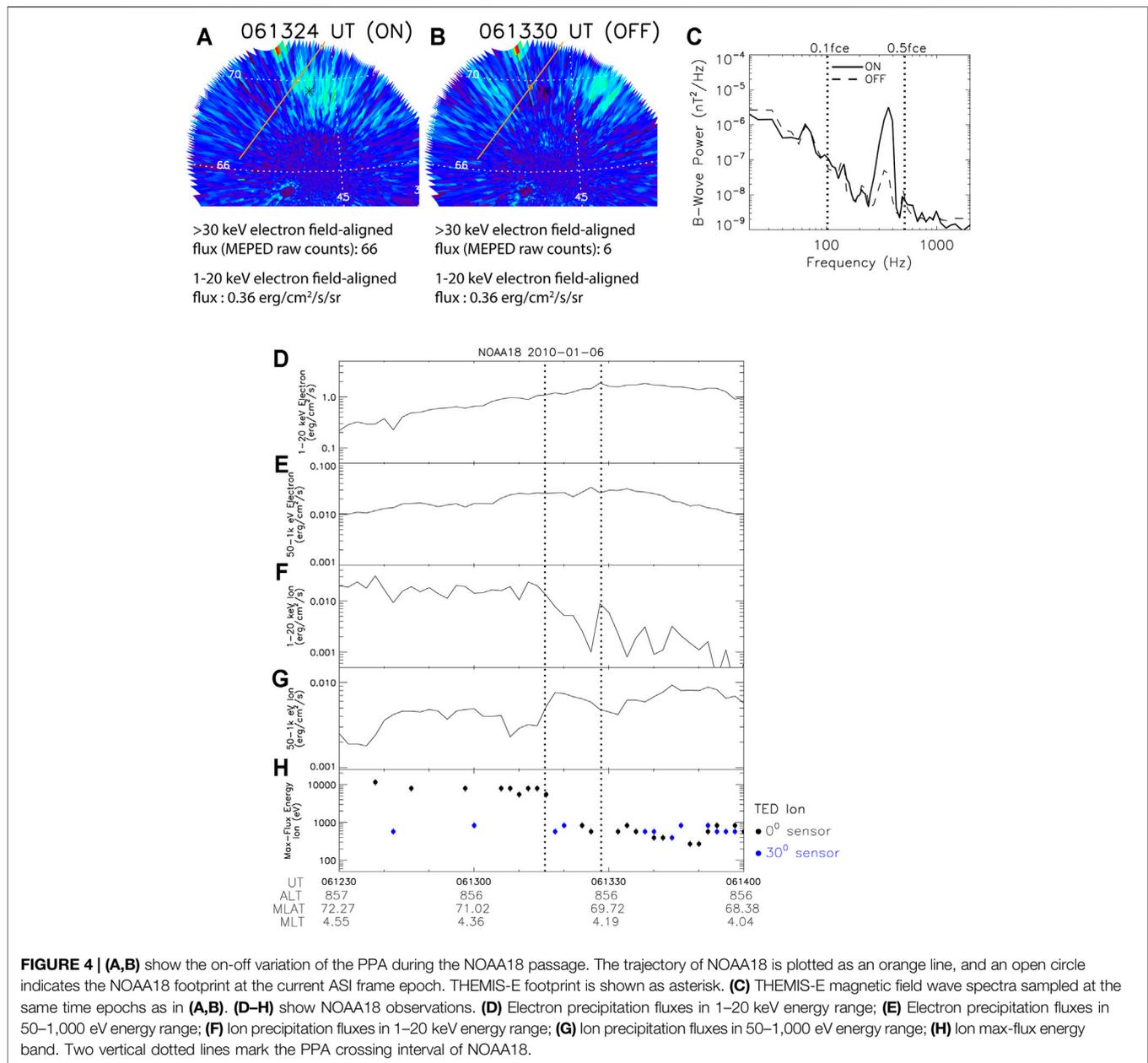
asterisk. **Figures 2C,F** show the FFT wave spectra of the THEMIS-E magnetic field (Roux et al., 2008) sampled at the same time epochs as in **Figures 2A,B,D,E**, respectively. The variation of the lower-band chorus wave, characterized by a distinct power peak within the frequency range 0.1–0.5 f_{ce} (electron gyrofrequency), is in concert with the on-off pulsation of the PPA, revealing an inherent link between them. To examine the presence/absence of such a PPA-chorus correlation over an extended interval, we first calculate the PPA luminosity in each ASI frame by averaging the raw counts within a box region encompassing the PPA region of interest (see red boxes in the plot); such a box region may be slightly shifted every 2 min to accommodate the slow motion of the patch during the event interval. We then calculate the chorus intensities on THEMIS-E by integrating the magnetic wave spectra over the frequency range 0.1–0.5 f_{ce}, and resample them at ASI frame epochs. The temporal variations of the PPA luminosity and the chorus intensity resulting from the above procedures are shown in **Figure 2G**. We then compute the correlation coefficients (**Figure 2H**) between them in a sliding time window with 2-min in windows length and 1-min as sliding step. Both the PPA

and the chorus waves persist over extended time intervals, but the PPA-chorus correlation is poor before ~0612 and after ~0623 UT, yet reasonably good between 0612 and 0623 UT. In line with Nishimura et al. (2011a; 2011b), we interpret the presence/absence of PPA-chorus correlation as indicative of whether THEMIS-E is situated inside/outside the PPA-associated flux tubes. According to the above observations and arguments, we evaluate that the TH-E traverses the PPA-associated flux tubes during ~0612–0623 UT.

Figure 3 displays the THEMIS-E particle observations (McFadden et al., 2008). Panels **Figures 3A–C** show the electron energy flux spectrograms in the perpendicular (75–105° pitch angle), parallel (0–15° pitch angle), and anti-parallel (165–180° pitch angle) directions, respectively. In each panel we have combined the ESA data in 5–25 keV energy range and the SST data in >28 keV energy range. There is a gradual rise of ≥30 keV electron fluxes with perpendicular fluxes distinctly higher than parallel/antiparallel fluxes after ~6 UT. It is reasonable to conceive that the enhanced flux and anisotropy of high-energy electrons may provide a free energy source for the growth of whistler-mode chorus, as well as contribute to a main part of the precipitation flux spectra when they are scattered by chorus waves. However, the rise of the energetic electron fluxes is gradual, and no high-energy electron structure can be specifically associated with the patch.

Figure 3D shows the ion energy flux spectrogram in the perpendicular direction. Except for the CPS thermal population, ion perpendicular fluxes at energies below 1 keV are very weak. **Figures 3E,F** offer the most important aspect of THEMIS observations of our interest in this paper. As one can see, the parallel and antiparallel fluxes are prevalent below 1 keV, and contain a number of energy-band-limited structures. We particularly highlight that the patch crossing interval is accompanied by a bi-directional low-energy field-aligned ion structures with energy band ~400–800 eV. The bottom panel of **Figure 4** shows the pitch-angle spectrogram of these 400–800 eV ions; they feature a field-aligned beam-like structure, and exist near-symmetrically in both parallel and anti-parallel directions.

In this event, a Polar Operational Environmental Satellite (POES), NOAA18, also traversed the PPA of interest at ~850 km altitude. To aid readers we shall first briefly introduce the instruments onboard NOAA18. The Total Electron Detector (TED) instrument measures the particle precipitation fluxes in two energy ranges, one between 1 and 20 keV, and the other between 50 and 1,000 eV. TED has two sensors: a 0°-sensor mounted to view roughly along the radial vector of the probe, and a 30°-sensor mounted to view in a direction 30° of the zenith. At auroral latitudes both sensors are well within the loss cone, and a total precipitation flux is evaluated from the directional fluxes in these two sensors. TED also records the particular energy band in the full range 50–20,000 eV that contains the maximum differential energy flux for the two sensors. TED has a limited capability of measuring differential energy fluxes in up to five energy bands, one from the max-flux energy band and others from four fixed energy bands in a low
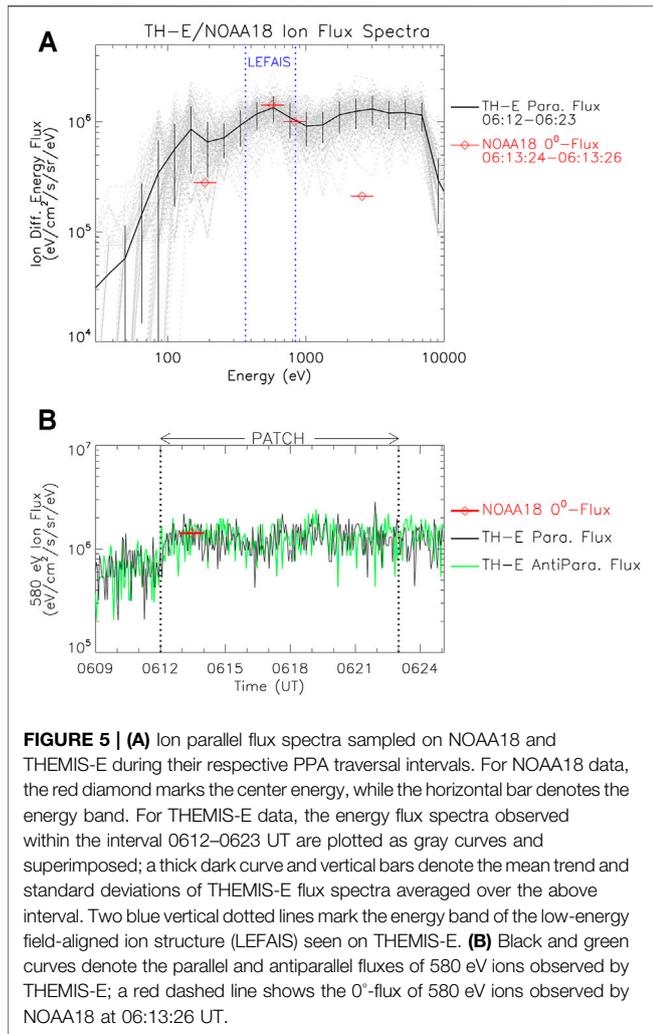
FIGURE 4 | (A,B) show the on-off variation of the PPA during the NOAA18 passage. The trajectory of NOAA18 is plotted as an orange line, and an open circle indicates the NOAA18 footprint at the current ASI frame epoch. THEMIS-E footprint is shown as asterisk. **(C)** THEMIS-E magnetic field wave spectra sampled at the same time epochs as in **(A,B)**. **(D–H)** show NOAA18 observations. **(D)** Electron precipitation fluxes in 1–20 keV energy range; **(E)** Electron precipitation fluxes in 50–1,000 eV energy range; **(F)** Ion precipitation fluxes in 1–20 keV energy range; **(G)** Ion precipitation fluxes in 50–1,000 eV energy range; **(H)** Ion max-flux energy band. Two vertical dotted lines mark the PPA crossing interval of NOAA18.

duty cycle. For more technical details and data processing procedures of POES data, see Liang et al. (2015).

Figures 4A,B display two auroral images at 06:13:24 and 06: 13:30 UT, showing the on-off variation of the PPA surrounding the passage of NOAA18, and the THEMIS-E wave spectra sampled at the two time epochs. Though in the following we shall focus more on the ion signatures associated with the PPA, we have also checked the electron flux data on NOAA18 and noticed that, the >30 keV electron field-aligned flux, obtained from the 0^0-sensor of the Medium Energy Proton and Electron Detector (MEPED), drops by an order of magnitude over the on-off transition of the PPA, yet the 1–20 keV electron flux observed by the TED is much less changed (see **Figure 4D**). The above observations suggest that high-energy (>20 keV) electrons might

contribute to a main portion of the modulated precipitation fluxes corresponding to the PPA in this event.

Figures 4D–H shows the NOAA18 TED observation. According to the patch dimension defined at its on-time, e.g., 06:13:24 UT, we estimate the interval when NOAA18 crossed the PPA, and mark it by vertical lines. The TED electron fluxes (**Figures 4D,E**) do not show appreciable variations across the patch in both 1–20 keV and 50–1,000 eV energy ranges. The ion flux variations are much more pronounced: the PPA occurs at a downslope of 1–20 keV ion precipitation fluxes (**Figure 4F**), yet is collocated with a peak of 50–1,000 eV ion precipitation fluxes (**Figure 4G**). Upon entering the PPA, the ion characteristic energy where the differential energy flux maximizes (**Figure 4H**) drops abruptly from ~10 keV (the CPS thermal

FIGURE 5 | (A) Ion parallel flux spectra sampled on NOAA18 and THEMIS-E during their respective PPA traversal intervals. For NOAA18 data, the red diamond marks the center energy, while the horizontal bar denotes the energy band. For THEMIS-E data, the energy flux spectra observed within the interval 0612–0623 UT are plotted as gray curves and superimposed; a thick dark curve and vertical bars denote the mean trend and standard deviations of THEMIS-E flux spectra averaged over the above interval. Two blue vertical dotted lines mark the energy band of the low-energy field-aligned ion structure (LEFAIS) seen on THEMIS-E. **(B)** Black and green curves denote the parallel and antiparallel fluxes of 580 eV ions observed by THEMIS-E; a red dashed line shows the 0°-flux of 580 eV ions observed by NOAA18 at 06:13:26 UT.

ions) to ~500–800 eV. The above features are consistent with those of the low-energy ion structure observed in Liang et al. (2015) as addressed in the previous subsection. Some lower-energy ions exist further equatorward over a broader MLAT width, possibly owing to some larger-scale warm cloak ions, but the high-energy electron fluxes (inferred from MEPED) become very weak there and thus no corresponding PPA is found.

We have shown that the low-energy ion structures associated with the PPA are identified in both the magnetosphere and the topside ionosphere in this event, which implies that the PPA-associated flux tubes are populated by such low-energy ion structures. According to Liouville's theorem, the field-aligned flux of the low-energy ion structure should be roughly conserved along the flux tube. To verify this, we collect the ion directional flux data from the 0°-sensor onboard NOAA18 as a proxy of the parallel flux. For THEMIS ESA measurements, we use the directional flux from the angular bin closest to the ambient magnetic field direction to approximate the parallel flux. **Figure 5** shows: a) superimposed THEMIS-E parallel flux spectra sampled during the patch crossing interval 0612–0623 UT, as well as their averaged trend; b) the temporal variations of

~580 eV ion parallel/antiparallel fluxes seen by THEMIS-E. The NOAA-18 parallel flux spectra and ~580 eV parallel flux level at its patch traversal epoch are overplotted. On average, the low-energy field-aligned ion structure measured by THEMIS-E matches well with that seen on NOAA18, in terms of both the max-flux energy (~580 eV) and the flux intensity at this energy. There is also close proximity between the ~850 eV ion flux seen on THEMIS-E and that on NOAA18, but the ion fluxes at ~3 keV and ~190 eV seen on NOAA18 are much lower than those measured on THEMIS-E. These observations indicate the presence of an energy-band-limited (~400–800 eV) low-energy ions flowing along the flux tubes threading the patch, which provides direct observational support to the scenario that the PPA connects to flux tubes filled with a low-energy plasma structure.

3.6 Possible Origin of the Field-Aligned Low-Energy Ion Structure

Liang et al. (2015) and Nishimura et al. (2015) both proposed that the ionospheric outflows are the likely source of low-energy ion structures in their observations, and that the outflows form the flux tubes with enhanced low-energy plasma that connect to the PPA. The ionospheric outflows would become a field-aligned beam structure in the magnetosphere due to the change of the magnetic field, though their pitch-angle distribution might be broadened by some processes, e.g., interaction with Alfven waves or other ULF waves (Li et al., 1997), leading the outflows to become partially trapped in the magnetosphere [see e.g., Welling et al. (2015)]. A bi-directional field-aligned distribution was found to be a common feature for ions with energies below several hundred eV in the near-Earth CPS (Wang et al., 2012). In a general sense, those field-aligned low-energy ions can be broadly categorized as "warm cloak plasma" in a classification of the cold plasma populations in the Earth's magnetosphere (Chappell, et al., 2008; Borovsky and Valdivia, 2018; Delzanno et al., 2021). In a nutshell, the warm plasma cloak consists of ions with energies of a few eV to greater than several hundred eV which display a characteristic bidirectional field-aligned pitch angle distribution. It is now well established that the ions in the warm plasma cloak owe their sources in the ionosphere, e.g., polar winds and auroral ion outflows. The occurrence distribution of warm cloak ions in the nightside (L~5–10 in the postmidnight-morning sector) overlaps with that of the PPAs (Chappell et al., 2008; Grono and Donovan, 2020).

That being said, we argue that the observed PPA-associated field-aligned low-energy ion structures may be different from the ambient warm plasma cloak ions, the latter of which owe their primary source from polar winds and are formed through stepwise energization processes in the polar cap and magnetotail (Chappell, et al., 2008). Instead, we speculate that the main source of the ~100 eV low-energy ion structures observed in Liang et al. (2015) and Nishimura et al. (2015) is likely auroral suprathermal ion outflows. Pulsating auroras usually occur during the later expansion phase and/or the recovery phase of a substorm (Jones et al., 2011; Partamies et al., 2017). Since auroral ion outflows often tend to be more structured and much more energetic than polar wind [e.g.,

Huddleston et al. (2005); Peterson et al. (2006); Welling et al. (2015)], the auroral ion outflows associated with the substorm intensification would add to the ambient warm cloak ions originating from the polar wind, and produce smaller-scale structures with above-par density and energy range over the ambient warm plasma cloak.

3.7 Indirect Clues of the Possible Existence of Low-Energy Electrons Associated With PPA

As addressed in the previous subsections, reliable detection of low-energy electrons and proper evaluation of their density remain to be challenging issues in practical *in-situ* observations to date. That said, there is indirect observational evidence that may allude to the possible existence of low-energy electrons associated with PPA. Liang et al. (2017; 2018) investigated the electron temperature (T_e) enhancement in the upper/topside ionosphere associated with PPAs. Based upon Swarm satellite measurements (Liang et al., 2017) and Poker Flat Incoherent Scatter Radar (PFISR) measurements (Liang et al., 2018), a strong T_e enhancement in the region of PPAs is found. The pulsating auroral precipitation itself that produces the optical luminosity usually consists of ~10 keV or even higher-energy electrons, which is ineffective in heating electrons in the upper/topside ionosphere. Instead, via model simulations Liang et al. (2017) reached a conclusion that, to account for realistic T_e observations in PPA events, the pulsating aurora is likely accompanied by a magnetospheric heat flux input distinctly higher than the typical ambient level of heat fluxes in the midnight-postmidnight ionosphere. It is reasonable to speculate that the heat flux leading to the observed T_e enhancement might be pertinent to certain specific mechanism of pulsating auroras. The heat flux is known to be led by the collisions between low-energy electrons (≤~10 eV) from the magnetosphere and the thermal electrons in the topside ionosphere. [e.g., Rees and Roble (1975)]. Under such a notion, the extra heat flux that results in the T_e enhancement related to PPA may allude to the potential existence of enhanced low-energy electron population extending from the magnetosphere to the upper boundary of the ionosphere in the PPA flux tubes.

4 DISCUSSION AND EXISTING THEORIES

While the phenomena of pulsating auroras have been known and extensively studied for decades, their generation mechanisms remain unclear and controversial to date. As correctly pointed out by Humberset et al. (2016), one problem that has confounded the exploration of the pulsating auroral mechanisms lies in that, there are probably many different types of auroral phenomena that have been mixed under the broad name of "pulsating auroras". Historically, pulsating auroras were subcategorized by Royrvik and Davis (1977) into patches, arcs, and arc segments, but modern literature generally only refers to "pulsating aurora" and "pulsating auroral patches" and would

not consider the "streaming arc" of Royrvik and Davis (1977) to be a type of pulsating aurora. On the other hand, omega bands have been observed to be accompanied by pulsating aurora (Partamies et al., 2017; Sato et al., 2015; 2017). Such omega-band pulsating auroras are less frequent than normal pulsating auroras embedded in ambient diffuse auroras, and it is not clear that the former share the same generation mechanism as the latter—Sato et al. (2015; 2017) proposed that DC electric field variation and low-frequency electrostatic waves, instead of the whistler-mode chorus, may play important roles in the driving mechanism of omega band pulsating auroras. However, their satellite measurements were far from the equator and thus the equatorial wave activity was unknown. The recent differentiation of pulsating auroras into APA and PPA alludes to possible differences in their generation mechanisms. Most importantly, the APA appears not to be necessarily related to enhanced cold plasma structure in the magnetosphere. In this review, we focus our interest on classical PPAs that are embedded in ambient diffuse auroras and characterized by their persistent shape over the order of ~10 min, and their motion velocity approximately conformal to E × B convection. In passing, we note that many of the following discussions about PPA would also be applicable to the non-pulsating PDA. According to current understandings (Grono and Donovan, 2020), PDA likely shares the same precipitation mechanism as PPA and is also hypothesized to map to a low-energy plasma structure in the magnetosphere, but differs from PPA only in the lack of the modulation of electron precipitation.

The generation mechanisms of PPA contains three separate yet inter-related modules: 1) the precipitation mechanism, namely what process drives the energetic electrons into the loss cone, which then precipitate into the Earth's atmosphere; 2) the patch shaping mechanism, namely what process defines the patch shape and size; 3) the modulation mechanism, namely what process modulates the precipitation mechanism within the patch. The pulsating aurora is usually classified as diffuse aurora (Nishimura et al., 2020). It is generally conceived to result from the pitch-angle scattering of energetic electrons into the loss cone by certain ELF/VLF waves. In the following discussions, we shall follow this standard notion. This does not mean that we deem the ELF/VLF wave scattering as the only viable precipitation mechanism for pulsating auroras, and we do realize the existence of counter-arguments/counter-examples and other suggested precipitation mechanisms [e.g., Sato et al. (2004; 2015); Nishiyama et al. (2012); Mozer et al. (2017)]. Nevertheless, it is fair to state that the ELF/VLF wave scattering scenario remains to be the top candidate mechanism to date (Nishimura et al., 2018) and has been experimentally supported by various reports based upon good correlations between the auroral pulsations and the temporal oscillations of magnetospheric chorus waves or ECH waves (Nishimura et al., 2010, 2011b; Ozaki et al., 2015; Fukizawa et al., 2018; Kasahara et al., 2018; Hosokawa et al., 2020). Another practical reason for us to focus our attention on the ELF/VLF wave scattering mechanism is to help us thread our following discussions to avoid being too much diversified. Known ELF/VLF wave modes that are linked to diffuse auroral

precipitation are the whistler-mode chorus (both lower-band and upper-band) and the ECH wave (Throne et al., 2010; Zhang et al., 2015; Ni et al., 2016). We shall use the whistler-mode chorus, the more prevalent one at play in pulsating auroras, in most of our subsequent discussion, and note that many of the following arguments would be equally applicable to ECH waves. For some arguments specific to ECH waves, we shall explicitly annotate.

The process(es) that control and determine the spatial dimension and size of PPA is not entirely clear to date, yet some reasonable inferences can be deducted from available observations and knowledge on the wave-particle interaction process. Given the notion that the pulsating aurora precipitation results from pitch-angle scattering of CPS energetic electrons into the loss cone by chorus waves, the question then becomes what parameters/processes cause the loss-cone flux of energetic electrons in one specific area to be higher than that in its ambient surrounding. The loss-cone flux is dependent upon the trapped energetic electron fluxes and the pitch-angle scattering rate. The salient patch properties such as its persistence in shape and overall $E \times B$ drift generally invalidate the possibility that the patch size is defined by an energetic electron structure. The cold electron density then naturally arises as one topmost candidate of what defines the patch structure. The cold electron density is known to be capable of influencing almost all the properties of the generated waves: frequency, growth rate, and saturation amplitude [e.g., see a review in Delzanno et al. (2021)]. Contingent upon the other plasma/wave parameters, a density enhancement or a density depletion may cause either an increase or a decrease of the wave growth rate. Furthermore, when the density enhancement/depletion is not confined to the equator but distributed along the flux tube, which is often the case for cold plasma in the inner magnetosphere, the flux tube with enhanced/depleted plasma density would act as a duct for whistler-mode wave propagation [e.g., Katoh, (2014)]. Ke et al. (2021) numerically investigated the whistler-mode wave trapped by a field-aligned density enhancement duct, and found that the duct-trapped whistler-mode waves may remain quasi-parallel and usually get much larger amplitudes than those unducted whistler waves during propagation away from the magnetic equator. The equatorial cold plasma density is also known to affect the growth of ECH waves [e.g., Liu et al. (2018)], though a field-aligned ducted propagation scenario may not apply to ECH since ECH waves are more confined to the equator (Meredith et al., 2009; Ni et al., 2011; Zhang et al., 2015).

While the role of cold electrons in the growth/propagation of chorus waves is theoretically well recognized, it remains a challenging issue to reliably measure the density of cold electrons on *in-situ* particle detectors. In many cases, the energy range of such cold electrons may be close to even below the satellite potential and/or the low-energy bound of *in-situ* particle instruments. For a comprehensive review on the current difficulties in measuring the cold plasma density and serval existing attempts to overcome the difficulties, see Delzanno et al. (2021). That being stated, a few progresses have been made in examining the hypothesis of PPA

connecting to a low-energy plasma structure in realistic observations. In this paper we have reviewed some existing reports in the above regard. At the time being, it seems that there is more supporting evidence that PPA is connected to a density-enhancement structure, consistent with the theoretical expectation under the circumstance that the low-energy plasma density is smaller than the hot plasma density (Cuperman and Landau, 1974; Wu et al., 2013; Nishimura et al., 2015), though the scenario of density-depletion PPA structure cannot be excluded. While the "warm plasma cloak" is known to be a common and large-scale feature in the postmidnight CPS (Chappell et al., 2008), the question is what extra sources/processes make the low-energy plasma have a structural dimension similar to that of PPAs. Liang et al. (2015) and Nishimura et al. (2015) both proposed that ionospheric auroral outflows may constitute one plausible formation mechanism of the flux tubes with enhanced cold plasma structure. There are of course other possible sources of the low-energy plasma structure in the magnetosphere. For example, the plasmaspheric plume, which is originally a plasmaspheric population, has known to be an important supplier of cold plasma in the outer magnetosphere (Chappell et al., 1970; Borovsky and Denton, 2008; Borovsky et al., 2013). The plume ions tend to have a perpendicular pitch-angle distribution, different from the field-aligned distribution of ionospheric outflows. However, in the postmidnight-dawn sector (>~3 MLT) auroral latitudes where PPAs are often found (Grono and Donovan, 2020), the occurrence probability of plasmaspheric plumes is fairly low (Moldwin et al., 2004; Darrouzet et al., 2008), leaving it a less likely candidate mechanism, as compared to auroral outflows, of the low-energy plasma structures shaping the PPA. At last, Liang et al. (2010) proposed that, in some cases magnetospheric ULF waves may spatially modulate the ambient low-energy plasma and generate density enhancement/depletion structures with spatial scales similar to the PPA dimension mapped to the magnetosphere.

We are then confronted with the central yet most puzzling question of pulsating auroras: what process(es) modulate the pulsating auroral precipitation. As pointed out by Humberset et al. (2016), there is so far a lack of satisfactory theories that can explain the nature of pulsating auroral modulation. Early in pulsating auroral studies, Coroniti and Kennel (1970) postulated that variations in the equatorial magnetic field, which in turn affected the strength of the ELF/VLF waves at play, are the cause of pulsating auroras. However, later observations in general invalidated such a hydromagnetic wave theory (Oguti et al., 1986; Li et al., 2011b; Nishimura et al., 2011; 2015). In many reported cases, when quasi-periodic modulation of chorus wave intensity at typical pulsating auroral periods (a few to a few tens of seconds) is observed, the oscillations of co-located electric/magnetic fields are found to be either trivial only or uncorrelated with the chorus wave modulation. This is in contrast to the observation that, modulation of whistler-mode chorus is often found in good correlation with longer-period (Pc4/Pc5) ULF waves (Li et al., 2011a; Jaynes et al., 2015).

The relaxation oscillator theory put forth by Davidson and Chiu (1987) and Davidson (1990) resorts to the nonlinear

feedback interaction between the pitch-angle anisotropy and the ELF/VLF wave growth. The picture is this: a particle distribution with a loss cone exists near the equator. Its pitch angle anisotropy favors a plasma instability that results in the generation of certain ELF/VLF waves which act to pitch-angle-scatter the electrons into the loss cone. Removal of the anisotropy reduces the growth of the waves. The loss cone is ultimately re-established when the electrons precipitate and are lost in the Earth's atmosphere, allowing the cycle to repeat. The nonlinearities inherent in the mechanism mean that in certain parameter regimes the interaction can act as a relaxation oscillator and yield quasi-periodic solutions, i.e., the auroral pulsation. The concept of the above theory seems to fit particularly well to ECH waves whose growth rate is controlled by the loss-cone distribution (Horne and Thorne, 2000; Zhang et al., 2015; Liu et al., 2018). Using their model Davidson and Chiu (1987) found that a small increase of as little as ~1% in cold plasma density can change the nonlinear system into a quasi-periodic regime. Unfortunately, the existing version of the relaxation oscillator theory remained heuristic to date. The intent of the theory was to describe a complicated physical system by a set of simple nonlinear equations, without becoming involved in the microphysics of the precise interaction mechanism. The appropriate physical parameters remained rather vaguely defined in the existing version of the theory.

Demekhov and Trakhtengerts (1994) proposed a theory which they dubbed the "flow cyclotron maser." Their theory suggested that a flux tube with enhanced cold plasma density can act as a resonance cavity for whistler-mode waves. The pulsating aurora is driven by a spike-like regime of whistler cyclotron instability (WCI) and in turn impulsive precipitation of energetic electrons in the duct with enhanced cold plasma density. Conceptually similar to the relaxation oscillator theory, the spike-like regime of WCI results from a nonlinear feedback interaction between the wave-driven pitch-angle diffusion and the growth rate of WCI (Trakhtengerts et al., 1986). Conditions for WCI to develop in a plasma duct depend strongly on the effective reflection coefficient at the edge of duct, and thus require a substantial difference between the plasma density inside of, and outside of, the PPA flux tube [$N_{inside} \geq 2N_{outside}$ as pointed out in Nemzek et al. (1995)]. Compared to the Davidson relaxation oscillator theory, the flow cyclotron maser theory dealt explicitly with the details of the wave-particle interactions, making the latter easier in some ways to compare with realistic observations. However, existing reports have directly indicated (Nemzek et al., 1995) or indirectly implied (Nishiyama et al., 2014; Nishimura et al., 2015) that the plasma density enhancement required by the flow cyclotron maser theory might not be satisfied in the realistic observations. Furthermore, Humberset et al. (2016) also found that Demekhov and Trakhtengerts (1994) model prediction of the on- and off-timescale may not fit the realistic observations.

Both the relaxation oscillator theory and the flow cyclotron maser theory postulate nonlinear dynamics as the cause of the modulation of ELF/VLF waves. They do not necessarily require time-oscillating cold plasma density for the wave modulation, though a region of enhanced cold plasma density is deemed as the necessary condition for those nonlinear dynamics to operate and produce solutions characteristic of PPA. On the other hand, Li

et al. (2011b) and Nishimura et al. (2015) both noticed that the modulation of whistler-mode chorus with repetitive periods similar to that of pulsating auroras appears to be correlated with the concurrent low-energy plasma density variations. A theory is thus proposed that the low-energy plasma density may directly modulate the growth rate of the chorus. In contrast, no evident correlation is found between such chorus modulation and the variations of the CPS thermal plasma density and the local electric/magnetic fields. The low-energy electron/ion structures corresponding to those density enhancement variations were found to feature a field-aligned anisotropy (Li et al., 2011b; Nishimura et al., 2015). Nishiyama et al. (2014) also suggested that the temporal variation in cold plasma density is the most plausible process behind the on-off auroral pulsations. Under the notion that the overall patch corresponds to a spatial structure of density enhancement/depletion, if it is the case that the low-energy plasma density variations directly modulate the chorus intensity, such temporal variations are likely superimposed on the overall spatial density structure. This is evidenced by the observations in Nishimura et al. (2015) that, the density variations that modulate the chorus intensity appear as fine-scale fluctuations superimposed on a field-aligned ion beam structure.

One shortcoming of the existing theoretical studies regarding the modulation of chorus waves by density variations (Li et al., 2011b; Nishimura et al., 2015) lies in that, the wave growth rate was evaluated locally at the equator only. For a field-aligned plasma structure, its density tends to be minimum at the magnetic equator. Consequently, the low-energy plasma density inferred from the equatorial magnetospheric observations is often small, so is its modulation on the local growth rate of chorus waves [e.g., Nishimura et al. (2015)]. It is not clear that the small variations of the local chorus growth rate as shown in Nishimura et al. (2015) would produce pronounced on-off auroral pulsations. The other question is the origin of such lower-energy plasma density fluctuations. The field-aligned anisotropy of the corresponding electron/ion structures, and the lack of apparently correlated fluctuations in other local parameters (CPS thermal plasma density and the local electric/magnetic fields) in the chorus modulation region, imply that the low-energy plasma modulation presumably originates from some nonlocal processes. Unfortunately, the exploration of the origin of such density variations requires multi-point observations in the magnetosphere, which is so far pending. The lack of definite knowledge of the low-energy density profile along the flux tubes is also the major difficulty hindering Nishimura et al. (2015) from performing a full wave growth calculation along the ray paths.

While the above discussion is based upon the notion that the PPA is mainly caused by pitch-angle scattering of energetic electrons by ELF/VLF waves, which primarily occurs in the equatorial magnetosphere, we certainly do not write off the potential existence of one or more ionospheric or near-Earth processes that may act as a secondary control mechanism on the pulsating aurora. The possible role of ionospheric or near-Earth processes in pulsating auroras was addressed by a number of researchers (Stenbaek-Nielsen, 1980; Tagirov et al., 1999; Sato et al., 2004; Nishimura et al., 2015; Humberset et al., 2016; 2018).

For example, Tagirov et al. (1999) considered the effect of ionospheric feedback on the flow cyclotron maser model (Demekhov and Trakhtengerts, 1994). They suggested that, the enhanced ionospheric electron density led by the on-time pulsating auroral precipitation would increase the absorption of whistler-mode waves at the ionospheric end and thus decrease the wave reflection, therefore reducing the total wave energy in the plasma duct. This acts as a feedback quenching process and results in the off-time of the pulsating aurora. As the electron density decreases due to recombination, it allows waves to begin to grow once again. On the other hand, a number of existing studies suggested the possible existence of parallel electric fields on top of the ionosphere over the pulsating auroral region (Sato et al., 2004; Williams et al., 2006; Samara et al., 2015). Given the moderate FAC intensity associated with pulsating auroras (no more than a few $\mu A/m^2$, see Gillies et al. (2015); Liang et al. (2017)), the corresponding $E_{//}$, if existing, is presumably not strong enough to significantly affect the precipitation fluxes of high-energy electrons ($\geq\sim10$ keV) typical of pulsating auroras, but might considerably influence the plasma outflows from the ionosphere. Under such a notion, the $E_{//}$associated pulsating auroras might affect the cold electron density and in turn the ELF/VLF wave growth in the magnetosphere. Admittedly, the above proposals all remain speculative at the time being. Operative near-Earth processes in pulsating auroras remain vague to date, and there is so far a lack of quantitative theories/models taking into account the role of the near-Earth processes in the generation/modulation of pulsating auroras in the existing literature.

5 CONCLUSION AND FUTURE DIRECTIONS

Despite decades of pulsating auroral studies, it remains unclear what processes define the shape/size of a PPA, though a hypothesis that PPA might be connected to a structure of enhanced cold plasma in the magnetosphere has long been one of the classical cornerstones of existing PPA theories. In this paper, we review the up-to-date observational reports, either direct or indirect, on the potential association between the low-energy plasma structure and the PPA. Based on existing evidence, we tentatively suggest that ionospheric auroral outflows might constitute one possible formation mechanism for the long-hypothesized flux tubes with enhanced cold plasma that connect to the PPA. At last, we review existing theories of pulsating auroras, with particular focus and comments on the role of low-energy plasma in these theories. To date, it is fair to state that none of the existing theories are complete and mature enough to offer a quantitatively satisfactory explanation of the observed PPA characteristics. To proceed with the pursuing of the pulsating auroras mechanisms, we would suggest the following tasks and research directions in the future.

1. Advance in an accurate measurement of the cold plasma density. Reliable measurements of the cold ion and cold electron populations and their interpretation are notoriously difficult. At a workshop on Unsolved Problems of Magnetospheric Physics in 2015, the lack of direct measurements of low-energy electrons and ions was listed as one of about a dozen unsolved problems of magnetospheric physics (Denton et al., 2016). Given the importance of cold electrons in magnetospheric dynamics, new methods that can reliably suppress photoemission or that can robustly distinguish photoelectrons from the cold-electron fluxes need to be developed. This would be key to the approval or disapproval of the long-pending hypothesis that PPA is connected to flux tubes filled with enhanced cold plasma. Besides, multi-point observations at different latitudes in the magnetosphere are also desirable to deduce the origin of the cold plasma structure and its temporal variations.

2. Advance in theories of the underlying mechanisms of oscillating ELF/VLF waves in the magnetosphere. The oscillation may come from either a nonlinear mechanism or a quasi-linear modulation by external parameter(s). A nonlinear mechanism is typically built upon a nonlinear feedback interaction between the pitch-angle anisotropy of energetic electrons and the growth of ELF/VLF waves. However, two major nonlinear theories of pulsating auroras to date, the relaxation oscillator theory (Davidson and Chiu, 1987; Davidson, 1990) and the flow cyclotron maser theory (Demekhov and Trakhtengerts, 1994), are both incomplete and/or unsatisfactory to a certain degree. New efforts must be made to renew the nonlinear theories to incorporate the updated understanding of waves and plasma parameters in the pulsating auroral region based on recent observations and simulations. It is desirable that the new nonlinear theory would explicitly contain microphysics of the wave-particle interaction and make falsifiable predictions of the wave evolution details. Nonlinear wave-particle interaction is widely accepted as the key component of the growth of ELF/VLF waves in the magnetosphere, and our understanding of such nonlinearities has greatly advanced in recent decades [see e.g., a review in Tao et al. (2020)]. Meanwhile, current observation techniques have enabled a high-resolution analysis of both ELF/VLF wave elements and pulsating auroras [e.g., Ozaki et al. (2019)].

   For the quasi-linear modulation mechanism, the oscillation of ELF/VLF wave intensity is deemed to be modulated by the cold plasma density variation (Li et al., 2011b; Nishimura et al., 2015). However, in existing theoretical investigations along such a direction, the wave growth rate was evaluated locally at the equator only. For future theoretical development, convective growths along wave ray paths, taking into account the ducted propagation, should be calculated to examine whether the density structure can give significant wave amplification. To achieve this, profiles of enhanced densities along magnetic field lines must be properly modeled based upon the realistic context of the lower-energy plasma structure, e.g., originating from auroral outflows.

3. Certain auxiliary processes in the topside ionosphere or near-Earth region. As afore-addressed, while the main generation

mechanism of pulsating auroras likely resides in the equatorial magnetosphere, certain ionospheric or near-Earth processes may well act as a secondary control mechanism on the pulsating auroras. For example, certain near-Earth processes might affect the auroral outflows and their density distribution extending into the magnetosphere, and in turn affect the propagation/amplification of whistler-mode waves in the pulsating auroral flux tubes. That stated, no clear candidate of such ionospheric or near-Earth processes is well established to date, and consideration of their roles in the pulsating auroral mechanisms remains to be lacking or quantitative at best in the existing theories. More definitive observations of operative near-Earth processes in pulsating auroral events, as well as quantitative models/theories addressing the roles of these near-Earth processes in the modulation of ELF/VLF waves in the magnetosphere, are desirable research directions in the future.

AUTHOR CONTRIBUTIONS

JL and YN contributed to conception and design of the study. JL conducted the most data analyses and wrote the first draft of the manuscript. YN contributed to the contents and offered useful suggestions. BY aided in the data analyses. ED supervised this study and offered useful suggestions. VA

is the PI of the THEMIS mission that is mostly used in this study. All authors contributed to manuscript revision, read, and approved the submitted version.

ACKNOWLEDGMENTS

SUPPLEMENTARY MATERIAL

The Supplementary Material for this article can be found online at: https://www.frontiersin.org/articles/10.3389/fspas.2021.792653/full#supplementary-material

Supplementary Video 1 | Auroral movie recorded by THEMIS all-sky imager at Gillam, Canada, on 2012-10-23.

REFERENCES

Akasofu, S.-I., Meng, C.-I., and Kimball, D. S. (1966). Dynamics of the aurora-VI. *J. Atmos. Terrestrial Phys.* 28 (5), 505–511. doi:10.1016/0021-9169(66)90060-2

Angelopoulos, V. (2008). The THEMIS Mission. *Space Sci. Rev.* 141 (1-4), 5–34. doi:10.1007/s11214-008-9336-1

Bolmgren, K. (2017). *Time Dependence of Average Structure Size and Precipitation Energy in Pulsating aurora (Dissertation)*. Sweden: KTH Royal Institute of Technology. Available at: http://urn.kb.se/resolve?urn=urn:nbn:se:kth:diva-211561.

Borovsky, J. E., and Denton, M. H. (2008). A Statistical Look at Plasmaspheric Drainage Plumes. *J. Geophys. Res.* 113 (A9), a–n. doi:10.1029/2007JA012994

Borovsky, J. E., Denton, M. H., Denton, R. E., Jordanova, V. K., and Krall, J. (2013). Estimating the Effects of Ionospheric Plasma on Solar Wind/magnetosphere Coupling via Mass Loading of Dayside Reconnection: Ion-Plasma-Sheet Oxygen, Plasmaspheric Drainage Plumes, and the Plasma Cloak. *J. Geophys. Res. Space Phys.* 118 (9), 5695–5719. doi:10.1002/jgra.50527

Borovsky, J. E., and Valdivia, J. A. (2018). The Earth's Magnetosphere: A Systems Science Overview and Assessment. *Surv. Geophys.* 39 (5), 817–859. doi:10.1007/s10712-018-9487-x

Carpenter, D. L., and Anderson, R. R. (1992). An ISEE/Whistler Model of Equatorial Electron Density in the Magnetosphere. *J. Geophys. Res.* 97, 1097–1108. doi:10.1029/91JA01548

Chappell, C. R., Harris, K. K., and Sharp, G. W. (1970). The Morphology of the Bulge Region of the Plasmasphere. *J. Geophys. Res.* 75 (19), 3848–3861. doi:10.1029/JA075i019p03848

Chappell, C. R., Huddleston, M. M., Moore, T. E., Giles, B. L., and Delcourt, D. C. (2008). Observations of the Warm Plasma Cloak and an Explanation of its Formation in the Magnetosphere. *J. Geophys. Res.* 113 (A9), a–n. doi:10.1029/2007JA012945

Coroniti, F. V., and Kennel, C. F. (1970). Auroral Micropulsation Instability. *J. Geophys. Res.* 75 (10), 1863–1878. doi:10.1029/JA075i010p01863

Cuperman, S., and Landau, R. W. (1974). On the Enhancement of the Whistler Mode Instability in the Magnetosphere by Cold Plasma Injection. *J. Geophys. Res.* 79 (1), 128–134. doi:10.1029/ja079i001p00128

Dahlgren, H., Lanchester, B. S., Ivchenko, N., and Whiter, D. K. (2017). Variations in Energy, Flux, and Brightness of Pulsating aurora Measured at High Time Resolution. *Ann. Geophys.* 35, 493–503. doi:10.5194/angeo-35-493-2017

Darrouzet, F., De Keyser, J., Décréau, P. M. E., El Lemdani-Mazouz, F., and Vallières, X. (2008). Statistical Analysis of Plasmaspheric Plumes with Cluster/WHISPER Observations. *Ann. Geophys.* 26 (8), 2403–2417. doi:10.5194/angeo-26-2403-2008

Davidson, G. T., and Chiu, Y. T. (1987). A Nonlinear Model of Wave-Particle Interactions in the Trapped Radiation Belts: Auroral Pulsation Solutions. *Geophys. Res. Lett.* 14 (11), 1166–1169. doi:10.1029/gl014i011p01166

Davidson, G. (1990). The Supernatural Poems. *Space Sci. Rev.* 53 (1-2), 45–87. doi:10.1007/978-1-349-20497-7_4

Davis, T. N. (1971). Magnetospheric Convection Pattern Inferred from Magnetic Disturbance and Auroral Motions. *J. Geophys. Res.* 76, 5978–5984. doi:10.1029/ja076i025p05978

Delzanno, G. L., Borovsky, J. E., Henderson, M. G., Resendiz Lira, P. A., Roytershteyn, V., Welling, D. T., et al. (2021). The Impact of Cold Electrons and Cold Ions in Magnetospheric Physics. *J. Atmos. Solar-Terrestrial Phys.* 220, 105599. doi:10.1016/j.jastp.2021.105599

Demekhov, A. G., and Trakhtengerts, V. Y. (1994). A Mechanism of Formation of Pulsating Aurorae. *J. Geophys. Res.* 99 (A4), 5831–5841. doi:10.1029/93JA01804

Denton, M. H., Borovsky, J. E., Stepanova, M., and Valdivia, J. A. (2016). Preface: Unsolved Problems of Magnetospheric Physics. *J. Geophys. Res. Space Phys.* 121 (10), 783. doi:10.1002/2016JA023362

Fukizawa, M., Sakanoi, T., Miyoshi, Y., Hosokawa, K., Shiokawa, K., Katoh, Y., et al. (2018). Electrostatic Electron Cyclotron Harmonic Waves as a Candidate to Cause Pulsating Auroras. *Geophys. Res. Lett.* 45 (12), 668. doi:10.1029/2018GL080145

Fukuda, Y., Kataoka, R., Miyoshi, Y., Katoh, Y., Nishiyama, T., Shiokawa, K., et al. (2016). Quasi-periodic Rapid Motion of Pulsating Auroras. *Polar Sci.* 10, 183–191. doi:10.1016/j.polar.2016.03.005

Gillies, D. M., Knudsen, D., Spanswick, E., Donovan, E., Burchill, J., and Patrick, M. (2015). Swarm Observations of Field-aligned Currents Associated with Pulsating Auroral Patches. *J. Geophys. Res. Space Phys.* 120, 9484–9499. doi:10.1002/2015JA021416

Grono, E., and Donovan, E. (2019). Constraining the Source Regions of Pulsating Auroras. *Geophys. Res. Lett.* 46, 10267–10273. doi:10.1029/2019GL084611

Grono, E., and Donovan, E. (2018). Differentiating Diffuse Auroras Based on Phenomenology. *Ann. Geophys.* 36 (3), 891–898. doi:10.5194/angeo-36-891-2018

Grono, E., Donovan, E., and Murphy, K. R. (2017). Tracking Patchy Pulsating aurora through All-Sky Images. *Ann. Geophys.* 35 (4), 777–784. doi:10.5194/angeo-35-777-2017

Grono, E., and Donovan, E. (2020). Surveying Pulsating Auroras. *Ann. Geophys.* 38, 1–8. doi:10.5194/angeo-38-1-2020

Hanzelka, M., and Santolík, O. (2019). Effects of Ducting on Whistler Mode Chorus or Exohiss in the Outer Radiation belt. *Geophys. Res. Lett.* 46 (11), 5735–5745. doi:10.1029/2019gl083115

Horne, R. B., and Thorne, R. M. (2000). Electron Pitch Angle Diffusion by Electrostatic Electron Cyclotron Harmonic Waves: The Origin of Pancake Distributions. *J. Geophys. Res.* 105 (A3), 5391–5402. doi:10.1029/1999ja900447

Hosokawa, K., Miyoshi, Y., Ozaki, M., Oyama, S.-I., Ogawa, Y., Kurita, S., et al. (2020). Multiple Time-Scale Beats in aurora: Precise Orchestration via Magnetospheric Chorus Waves. *Sci. Rep.* 10, 3380. doi:10.1038/s41598-020-59642-8

Hosokawa, K., Ogawa, Y., Kadokura, A., Miyaoka, H., and Sato, N. (2010). Modulation of Ionospheric Conductance and Electric Field Associated with Pulsating aurora. *J. Geophys. Res.* 115 (A3), a–n. doi:10.1029/2009JA014683

Hosokawa, K., Sato, A., Bjornsson, N., SatoMilan, S. E., Lester, M., Bjornsson, G., et al. (2008). Electric Field Modulation behind Pulsating aurora. *J. Geophys. Res.* 113, a–n. doi:10.1029/2008JA013601

Huddleston, M. M., Chappell, C. R., Delcourt, D. C., Moore, T. E., Giles, B. L., and Chandler, M. O. (2005). An Examination of the Process and Magnitude of Ionospheric Plasma Supply to the Magnetosphere. *J. Geophys. Res.* 110 (A12), A12202. doi:10.1029/2004JA010401

Humberset, B. K., Gjerloev, J. W., Mann, I. R., Michell, R. G., and Samara, M. (2018). On the Persistent Shape and Coherence of Pulsating Auroral Patches. *J. Geophys. Res. Space Phys.* 123, 4272–4289. doi:10.1029/2017JA024405

Humberset, B. K., Gjerloev, J. W., Samara, M., Michell, R. G., and Mann, I. R. (2016). Temporal Characteristics and Energy Deposition of Pulsating Auroral Patches. *J. Geophys. Res. Space Phys.* 121, 7087–7107. doi:10.1002/2016JA022921

Jaynes, A. N., Lessard, M. R., Rodriguez, J. V., Donovan, E., Loto'aniu, T. M., and Rychert, K. (2013). Pulsating Auroral Electron Flux Modulations in the Equatorial Magnetosphere. *J. Geophys. Res. Space Phys.* 118, 4884–4894. doi:10.1002/jgra.50434

Jaynes, A. N., Lessard, M. R., Takahashi, K., Ali, A. F., Malaspina, D. M., Michell, R. G., et al. (2015). Correlated Pc4-5 ULF Waves, Whistler-mode Chorus, and Pulsating aurora Observed by the Van Allen Probes and Ground-based Systems. *J. Geophys. Res. Space Phys.* 120, 8749–8761. doi:10.1002/2015JA021380

Johnstone, A. D. (1978). Pulsating aurora. *Nature* 274, 119–126. doi:10.1038/274119a0

Jones, S. L., Lessard, M. R., Rychert, K., Spanswick, E., Donovan, E., and Jaynes, A. N. (2013). Persistent, Widespread Pulsating aurora: A Case Study. *J. Geophys. Res. Space Phys.* 118, 2998–3006. doi:10.1002/jgra.50301

Jones, S. L., Lessard, M. R., Rychert, K., Spanswick, E., and Donovan, E. (2011). Large-scale Aspects and Temporal Evolution of Pulsating aurora. *J. Geophys. Res.* 116, A03214. doi:10.1029/2010ja015840

Kangas, J., and Cao, C. (1995). Pulsating aurora --- a Review. *Chin. J. Polar Res.* 6, 39–50.

Kasahara, S., Miyoshi, Y., Yokota, S., Mitani, T., Kasahara, Y., Matsuda, S., et al. (2018). Pulsating aurora from Electron Scattering by Chorus Waves. *Nature* 554 (7692), 337–340. doi:10.1038/nature25505

Katoh, Y. (2014). A Simulation Study of the Propagation of Whistler-Mode Chorus in the Earth's Inner Magnetosphere. *Earth Planet. Sp* 66, 6. doi:10.1186/1880-5981-66-6

Ke, Y., Chen, L., Gao, X., Lu, Q., Wang, X., Chen, R., et al. (2021). Whistler-Mode Waves Trapped by Density Irregularities in the Earth's Magnetosphere. *Geophys. Res. Lett.* 48, e2020GL092305. doi:10.1029/2020GL092305

Khazanov, G. V., Glocer, A., and Himwich, E. W. (2014). Magnetosphere-ionosphere Energy Interchange in the Electron Diffuse aurora. *J. Geophys. Res. Space Phys.* 119, 171–184. doi:10.1002/2013JA019325

Knudsen, D. J., Burchill, J. K., Buchert, S. C., Eriksson, A. I., Gill, R., Wahlund, J. E., et al. (2017). Thermal Ion Imagers and Langmuir Probes in the Swarm Electric Field Instruments. *J. Geophys. Res. Space Phys.* 122, 2655–2673. doi:10.1002/2016JA022571

Lessard, M. R. (2012). "A Review of Pulsating Aurora," in *Auroral Phenomenology and Magnetospheric Processes: Earth and Other Planets*. Editors A. Keiling, E. Donovan, F. Bagenal, and T. Karlsson (Washington, D. C: American Geophysical Union). doi:10.1029/2011GM001187

Li, Y., Yoon, P. H., Wu, C. S., WeatherwaxIon, A. T., Chao, J. K., and Wu, B. H. (1997). Ion Pitch-Angle Scattering by Alfvén Waves. *Phys. Plasmas* 4, 4103–4117. doi:10.1063/1.872530

Li, W., Bortnik, J., Thorne, R. M., Nishimura, Y., Angelopoulos, V., and Chen, L. (2011b). Modulation of Whistler Mode Chorus Waves: 2. Role of Density Variations. *J. Geophys. Res.* 116, a–n. doi:10.1029/2010JA016313

Li, W., Thorne, R. M., Bortnik, J., Nishimura, Y., and Angelopoulos, V. (2011a). Modulation of Whistler Mode Chorus Waves: 1. Role of Compressional Pc4-5 Pulsations. *J. Geophys. Res.* 116 (A6), a–n. doi:10.1029/2010JA016312

Liang, J., Donovan, E., Jackel, B., Spanswick, E., and Gillies, M. (2016). On the 630 Nm Red-line Pulsating aurora: Red-line Emission Geospace Observatory Observations and Model Simulations. *J. Geophys. Res. Space Phys.* 121 (8), 7988–8012. doi:10.1002/2016JA022901

Liang, J., Donovan, E., Nishimura, Y., Yang, B., Spanswick, E., Asamura, K., et al. (2015). Low-energy Ion Precipitation Structures Associated with Pulsating Auroral Patches. *J. Geophys. Res. Space Phys.* 120, 5408–5431. doi:10.1002/2015JA021094

Liang, J., Donovan, E., Reimer, A., Hampton, D., Zou, S., and Varney, R. (2018). Ionospheric Electron Heating Associated with Pulsating Auroras: Joint Optical and PFISR Observations. *J. Geophys. Res. Space Phys.* 123, 4430–4456. doi:10.1029/2017JA025138

Liang, J., Uritsky, V., Donovan, E., Ni, B., Spanswick, E., Trondsen, T., et al. (2010). THEMIS Observations of Electron Cyclotron Harmonic Emissions, ULF Waves, and Pulsating Auroras. *J. Geophys. Res.* 115, a–n. doi:10.1029/2009JA015148

Liang, J., Yang, B., Donovan, E., Burchill, J., and Knudsen, D. (2017). Ionospheric Electron Heating Associated with Pulsating Auroras: A Swarm Survey and Model Simulation. *J. Geophys. Res. Space Phys.* 122, 8781–8807. doi:10.1002/2017JA024127

Liu, X., Chen, L., Gu, W., and Zhang, X. J. (2018). Electron Cyclotron Harmonic Wave Instability by Loss Cone Distribution. *J. Geophys. Res. Space Phys.* 123, 9035–9044. doi:10.1029/2018ja025925

Malaspina, D. M., Ergun, R. E., Sturner, A., Wygant, J. R., Bonnell, J. W., Breneman, A., et al. (2014). Chorus Waves and Spacecraft Potential Fluctuations: Evidence for Wave-Enhanced Photoelectron Escape. *Geophys. Res. Lett.* 41, 236–243. doi:10.1002/2013GL058769

McEwen, D. J., Yee, E., Whalen, B. A., and Yau, A. W. (1981). Electron Energy Measurements in Pulsating Auroras. *Can. J. Phys.* 59 (8), 1106–1115. doi:10.1139/p81-146

McFadden, J. P., Carlson, C. W., Larson, D., Ludlam, M., Abiad, R., Elliott, B., et al. (2008). The THEMIS ESA Plasma Instrument and In-Flight Calibration. *Space Sci. Rev.* 141, 277–302. doi:10.1007/s11214-008-9440-2

Meredith, N. P., Horne, R. B., Thorne, R. M., and Anderson, R. R. (2009). Survey of Upper Band Chorus and ECH Waves: Implications for the Diffuse aurora. *J. Geophys. Res.* 114, a–n. doi:10.1029/2009JA014230

Miyoshi, Y., Katoh, Y., Nishiyama, T., Sakanoi, T., Asamura, K., and Hirahara, M. (2010). Time of Flight Analysis of Pulsating aurora Electrons, Considering Wave-Particle Interactions with Propagating Whistler Mode Waves. *J. Geophys. Res.* 115, a–n. doi:10.1029/2009JA015127

Miyoshi, Y., Oyama, S., Saito, S., Kurita, S., Fujiwara, H., Kataoka, R., et al. (2015). Energetic Electron Precipitation Associated with Pulsating aurora: EISCAT and Van Allen Probe Observations. *J. Geophys. Res. Space Phys.* 120, 2754–2766. doi:10.1002/2014JA020690

Moldwin, M. B., Howard, J., Sanny, J., Bocchicchio, J. D., Rassoul, H. K., and Anderson, R. R. (2004). Plasmaspheric Plumes: CRRES Observations of Enhanced Density beyond the Plasmapause. *J. Geophys. Res.* 109, A05202. doi:10.1029/2003JA010320

Mozer, F. S., Agapitov, O. V., Hull, A., Lejosne, S., and Vasko, I. Y. (2017). Pulsating Auroras Produced by Interactions of Electrons and Time Domain Structures. *J. Geophys. Res. Space Phys.* 122, 8604–8616. doi:10.1002/2017JA024223

Nakamura, R., and Oguti, T. (1987). Drifts of Auroral Structures and Magnetospheric Electric fields. *J. Geophys. Res.* 92 (A10), 11241–11247. doi:10.1029/JA092iA10p11241

Nemzek, R. J., Nakamura, R., Baker, D. N., Belian, R. D., McComas, D. J., Thomsen, M. F., et al. (1995). The Relationship between Pulsating Auroras Observed from the Ground and Energetic Electrons and Plasma Density Measured at Geosynchronous Orbit. *J. Geophys. Res.* 100 (A12), 23935–23944. doi:10.1029/95JA01756

Ni, B., Thorne, R., Liang, J., Angelopoulos, V., Cully, C., Li, W., et al. (2011). Global Distribution of Electrostatic Electron Cyclotron Harmonic Waves Observed on THEMIS. *Geophys. Res. Lett.* 38, a–n. doi:10.1029/2011GL048793

Ni, B., Thorne, R. M., Zhang, X., Bortnik, J., Pu, Z., Xie, L., et al. (2016). Origins of the Earth's Diffuse Auroral Precipitation. *Space Sci. Rev.* 200, 205–259. doi:10.1007/s11214-016-0234-7

Nishimura, Y., Bortnik, J., Li, W., Angelopoulos, V., Donovan, E. F., and Spanswick, E. L. (2018). Comment on "pulsating auroras produced by interactions of electrons and time domain structures" by Mozer et al. *J. Geophys. Res. Space Phys.* 123, 2064–2070. doi:10.1002/2017JA024844

Nishimura, Y., Bortnik, J., Li, W., Liang, J., Thorne, R. M., Angelopoulos, V., et al. (2015). Chorus Intensity Modulation Driven by Time-varying Field-aligned Low-energy Plasma. *J. Geophys. Res. Space Phys.* 120, 7433–7446. doi:10.1002/2015JA021330

Nishimura, Y., Bortnik, J., Li, W., Thorne, R. M., Chen, L., Lyons, L. R., et al. (2011b). Multievent Study of the Correlation between Pulsating aurora and Whistler Mode Chorus Emissions. *J. Geophys. Res.* 116, a–n. doi:10.1029/2011JA016876

Nishimura, Y., Bortnik, J., Li, W., Thorne, R. M., Lyons, L. R., Angelopoulos, V., et al. (2011a). Estimation of Magnetic Field Mapping Accuracy Using the Pulsating aurora-chorus Connection. *Geophys. Res. Lett.* 38, a–n. doi:10.1029/2011GL048281

Nishimura, Y., Bortnik, J., Li, W., Thorne, R. M., Lyons, L. R., Angelopoulos, V., et al. (2010). Identifying the Driver of Pulsating Aurora. *Science* 330, 81–84. doi:10.1126/science.1193186

Nishimura, Y., Lessard, M. R., Katoh, Y., Miyoshi, Y., Grono, E., Partamies, N., et al. (2020). Diffuse and Pulsating Aurora. *Space Sci. Rev.* 216, 4. doi:10.1007/s11214-019-0629-3

Nishiyama, T., Miyoshi, Y., Katoh, Y., Sakanoi, T., Kataoka, R., and Okano, S. (2016). Substructures with Luminosity Modulation and Horizontal Oscillation in Pulsating Patch: Principal Component Analysis Application to Pulsating aurora. *J. Geophys. Res. Space Phys.* 121 (3), 2360–2373. doi:10.1002/2015ja022288

Nishiyama, T., Sakanoi, T., Miyoshi, Y., Hampton, D. L., Katoh, Y., Kataoka, R., et al. (2014). Multiscale Temporal Variations of Pulsating Auroras: On-Off Pulsation and a Few Hz Modulation. *J. Geophys. Res. Space Phys.* 119 (5), 3514–3527. doi:10.1002/2014JA019818

Nishiyama, T., Sakanoi, T., Miyoshi, Y., Kataoka, R., Hampton, D., Katoh, Y., et al. (2012). Fine Scale Structures of Pulsating Auroras in the Early Recovery Phase of Substorm Using Ground-Based EMCCD Camera. *J. Geophys. Res.* 117 (A10), a–n. doi:10.1029/2012JA017921

Nishiyama, T., Sakanoi, T., Miyoshi, Y., Katoh, Y., Asamura, K., Okano, S., et al. (2011). The Source Region and its Characteristic of Pulsating aurora Based on the Reimei Observations. *J. Geophys. Res.* 116, A03226. doi:10.1029/2010JA015507

Peterson, W. K., Collin, H. L., Lennartsson, O. W., and Yau, A. W. (2006). Quiet Time Solar Illumination Effects on the Fluxes and Characteristic Energies of Ionospheric Outflow. *J. Geophys. Res.* 111, A11S05. doi:10.1029/2005JA011596

Oguti, T., Hayashi, K., Yamamoto, T., Ishida, J., Higuchi, T., and Nishitani, N. (1986). Absence of Hydromagnetic Waves in the Magnetospheric Equatorial Region Conjugate with Pulsating Auroras. *J. Geophys. Res.* 91, 13711–13715. doi:10.1029/ja091ia12p13711

Oguti, T. (1976). Recurrent Auroral Patterns. *J. Geophys. Res.* 81 (10), 1782–1786. doi:10.1029/ja081i010p01782

Ozaki, M., Miyoshi, Y., Shiokawa, K., Hosokawa, K., Oyama, S.-i., Kataoka, R., et al. (2019). Visualization of Rapid Electron Precipitation via Chorus Element Wave-Particle Interactions. *Nat. Commun.* 10, 257. doi:10.1038/s41467-018-07996-z

Ozaki, M., Shiokawa, K., Miyoshi, Y., Hosokawa, K., Oyama, S., Yagitani, S., et al. (2018). Microscopic Observations of Pulsating Aurora Associated with Chorus Element Structures: Coordinated Arase Satellite-PWING Observations. *Geophys. Res. Lett.* 45 (22), 125–134. doi:10.1029/2018GL079812

Ozaki, M., Yagitani, S., Sawai, K., Shiokawa, K., Miyoshi, Y., Kataoka, R., et al. (2015). A Direct Link between Chorus Emissions and Pulsating aurora on Timescales from Milliseconds to Minutes: a Case Study at Subauroral Latitudes. *J. Geophys. Res. Space Phys.* 120, 9617–9631. doi:10.1002/2015JA021381

Partamies, N., Bolmgren, K., Heino, E., Ivchenko, N., Borovsky, J. E., and Sundberg, H. (2019). Patch Size Evolution during Pulsating aurora. *J. Geophys. Res. Space Phys.* 124, 4725–4738. doi:10.1029/2018JA026423

Partamies, N., Whiter, D., Kadokura, A., Kauristie, K., Nesse Tyssøy, H., Massetti, S., et al. (2017). Occurrence and Average Behavior of Pulsating aurora. *J. Geophys. Res. Space Phys.* 122, 5606–5618. doi:10.1002/2017JA024039

Rees, M. H., and Roble, R. G. (1975). Observations and Theory of the Formation of Stable Auroral Red Arcs. *Rev. Geophys.* 13 (1), 201–242. doi:10.1029/RG013i001p00201

Roux, A., Le Contel, O., Coillot, C., Bouabdellah, A., de la Porte, B., Alison, D., et al. (2008). The Search Coil Magnetometer for THEMIS. *Space Sci. Rev.* 141, 265–275. doi:10.1007/s11214-008-9455-8

Royrvik, O., and Davis, T. N. (1977). Pulsating Aurora: Local and Global Morphology. *J. Geophys. Res.* 82 (29), 4720–4740. doi:10.1029/ja082i029p04720

Samara, M., Michell, R. G., Asamura, K., Hirahara, M., Hampton, D. L., and Stenbaek-Nielsen, H. C. (2010). Ground-based Observations of Diffuse Auroral Structures in Conjunction with Reimei Measurements. *Ann. Geophys.* 28 (3), 873–881. doi:10.5194/angeo-28-873-2010

Samara, M., Michell, R. G., and Redmon, R. J. (2015). Low-altitude Satellite Measurements of Pulsating Auroral Electrons. *J. Geophys. Res. Space Phys.* 120, 8111–8124. doi:10.1002/2015JA021292

Sandahl, I., Eliasson, L., and Lundin, R. (1980). Rocket Observations of Precipitating Electrons over a Pulsating aurora. *Geophys. Res. Lett.* 7, 309–312. doi:10.1029/GL007i005p00309

Sato, N., Kadokura, A., Tanaka, Y., Nishiyama, T., Hori, T., and Yukimatu, A. S. (2015). Omega Band Pulsating Auroras Observed Onboard THEMIS Spacecraft and on the Ground. *J. Geophys. Res. Space Phys.* 120, 5524–5544. doi:10.1002/2015JA021382

Sato, N., Morooka, M., Minatoya, K., and Saemundsson, T. (1998). Nonconjugacy of Pulsating Auroral Patches Near L=6. *Geophys. Res. Lett.* 25, 3755–3758. doi:10.1029/1998gl900002

Sato, N., Wright, D. M., Carlson, C. W., Ebihara, Y., Sato, M., Saemundsson, T., et al. (2004). Generation Region of Pulsating aurora Obtained Simultaneously by the FAST Satellite and a Syowa-Iceland Conjugate Pair of Observatories. *J. Geophys. Res.* 109, A10201. doi:10.1029/2004JA010419

Sato, N., Yukimatu, A. S., Tanaka, Y., and Hori, T. (2017). Morphologies of omega Band Auroras. *Earth Planets Space* 69, 103. doi:10.1186/s40623-017-0688-1

Scourfield, M. W. J., Innes, W. F., and Parsons, N. R. (1972). Spatial Coherency in Pulsating aurora. *Planet. Space Sci.* 20, 1843–1848. doi:10.1016/0032-0633(72)90117-1

Scourfield, M. W. J., Keys, J. G., Nielsen, E., Goertz, C. K., and Collin, H. (1983). Evidence for theE×Bdrift of Pulsating Auroras. *J. Geophys. Res.* 88, 7983–7988. doi:10.1029/ja088ia10p07983

Sheeley, B. W., Moldwin, M. B., Rassoul, H. K., and Anderson, R. R. (2001). An Empirical Plasmasphere and Trough Density Model: CRRES Observations. *J. Geophys. Res.* 106, 25631–25641. doi:10.1029/2000JA000286

Stenbaek-Nielsen, H. C. (1980). Pulsating aurora: The Importance of the Ionosphere. *Geophys. Res. Lett.* 7, 353–356. doi:10.1029/GL007i005p00353

Tagirov, V. R., Ismagilov, V. S., Titova, E. E., Arinin, V. A., Perlikov, A. M., Manninen, J., et al. (1999). Auroral Pulsations and Accompanying VLF Emissions. *Ann. Geophys.* 17, 66–78. doi:10.1007/s00585-999-0066-9

Takahashi, T., Virtanen, I. I., Hosokawa, K., Ogawa, Y., Aikio, A., Miyoka, H., et al. (2019). Polarization Electric Field inside Auroral Patches: Simultaneous experiment of EISCAT Radars and KAIRA. *J. Geophys. Res. Space Phys.* 124, 3543–3557. doi:10.1029/2018JA026254

Tao, X., Zonca, F., Chen, L., and Wu, Y. (2020). Theoretical and Numerical Studies of Chorus Waves: A Review. *Sci. China Earth Sci.* 63, 78–92. doi:10.1007/s11430-019-9384-6

Tesema, F., Partamies, N., Nesse Tyssøy, H., and McKay, D. (2020). Observations of Precipitation Energies during Different Types of Pulsating aurora. *Ann. Geophys.* 38, 1191–1202. doi:10.5194/angeo-38-1191-2020

Throne, R. M., Ni, B., Tao, X., Horne, R. B., and Meredith, N. P. (2010). Scattering by Chorus Waves as the Dominant Cause of Diffuse Auroral Precipitation. *Nature* 467, 943–946. doi:10.1038/nature09467

Trakhtengerts, V. Y., Tagirov, V. R., and Chernous, S. A. (1986). Flow Cyclotron Maser and Impulsive VLF Emissions. *Geomagn. Aeron.* 26 (1), 99–106.

Viereck, R. A., and Stenbaek-Nielsen, H. C. (1985). Pulsating Aurora and Hydrogen Emissions. *J. Geophys. Res.* 90 (11), 035. doi:10.1029/ja090ia11p11035

Wang, C.-P., Zaharia, S. G., Lyons, L. R., and Angelopoulos, V. (2013). Spatial Distributions of Ion Pitch Angle Anisotropy in the Near-Earth Magnetosphere and Tail Plasma Sheet. *J. Geophys. Res. Space Phys.* 118, 244–255. doi:10.1029/2012JA018275

Watanabe, M., Kadokura, A., Sato, N., and Saemundsson, T. (2007). Absence of Geomagnetic Conjugacy in Pulsating Auroras. *Geophys. Res. Lett.* 34, L15107. doi:10.1029/2007gl030469

Welling, D. T., André, M., Dandouras, I., Delcourt, D., Fazakerley, A., Fontaine, D., et al. (2015). The Earth: Plasma Sources, Losses, and Transport Processes. *Space Sci. Rev.* 192 (1), 145–208. doi:10.1007/s11214-015-0187-2

Williams, J. D., Macdonald, E., Mccarthy, M., Peticolas, L., and Parks, G. K. (2006). Parallel Electric fields Inferred during a Pulsating aurora. *Ann. Geophys.* 24, 1829–1837. doi:10.5194/angeo-24-1829-2006

Wu, S., Denton, R. E., and Li, W. (2013). Effects of Cold Electron Density on the Whistler Anisotropy Instability. *J. Geophys. Res. Space Phys.* 118, 765–773. doi:10.1029/2012ja018402

Yamamoto, T. (1988). On the Temporal Fluctuations of Pulsating Auroral Luminosity. *J. Geophys. Res.* 93, 897–911. doi:10.1029/ja093ia02p00897

Yang, B., Donovan, E., Liang, J., Knudsen, D., Burchill, J., Kouznetsov, A., et al. (2014). Coordinated Swarm *In-Situ* and THEMIS All Sky Imager Observations of the Motion of Patchy Pulsating aurora. *Eos. Trans. AGU Fall Meeting, Suppl.* Gp44a-03.

Yang, B., Donovan, E., Liang, J., and Spanswick, E. (2017). A Statistical Study of the Motion of Pulsating aurora Patches: Using the THEMIS All-Sky Imager. *Ann. Geophys.* 35, 217–225. doi:10.5194/angeo-35-217-2017

Yang, B., Spanswick, E., Liang, J., Grono, E., and Donovan, E. (2019). Responses of Different Types of Pulsating aurora in Cosmic Noise Absorption. *Geophys. Res. Lett.* 46, 5717–5724. doi:10.1029/2019gl083289

Yang, B. (2017). *Using the Motion of Patchy Pulsating Aurora to Remote Sense Magnetospheric Convection (Unpublished Doctoral Thesis).* Calgary, AB: University of Calgary. doi:10.11575/PRISM/28621

Zhang, X.-J., Angelopoulos, V., Ni, B., and Thorne, R. M. (2015). Predominance of ECH Wave Contribution to Diffuse aurora in Earth's Outer Magnetosphere. *J. Geophys. Res. Space Phys.* 120, 295–309. doi:10.1002/2014JA020455